Master's thesis
Master's Programme in Materials Research
Polymer materials chemistry

SYNTHESIS AND SOLUTION PROPERTIES OF BLOCK POLYAMPHOLYTE

Kati Meriläinen

02.2020

Supervisor(s): Vikram Baddam

Examiner(s): Heikki Tenhu and Sami Hietala

UNIVERSITY OF HELSINKI
FACULTY OF SCIENCE

Tiedekunta – Fakultet – Faculty	Koulutusohjelma – Utbildningsprogram – Degree programme
Faculty of science	Master's Programme in Materials Research

Tekijä – Författare – Author
Kati Meriläinen

Työn nimi – Arbetets titel – Title
Synthesis and solution properties of block polyampholyte

Työn laji – Arbetets art – Level	Aika – Datum – Month and year	Sivumäärä – Sidoantal – Number of pages
Master's thesis	02.2020	49

Tiivistelmä – Referat – Abstract

In this thesis, synthesis and solution properties of the polyampholyte poly(acrylic acid)-b-poly[(vinylbenzyl)trimethylammonium chloride], PAA-PVBTMA-Cl, were investigated in aqueous solutions. First, the diblock copolymer was synthesized via RAFT polymerization where poly(acrylic acid), PAA was used as a chain transfer agent (CTA). In addition, the homopolymer poly[(vinylbenzyl)trimethylammonium chloride], PVBTMA-Cl, was synthesized via RAFT polymerization to compare the solution properties with the block copolymer. Molar masses of the polymers were determined using several methods such as NMR, UV-Vis spectroscopy and SEC. The experimental molar masses were close to theoretical values and block ratio in diblock copolymer from NMR was 30% of AA and 70% of VBTMA-Cl. Furthermore, the solution properties of the polyampholyte were studied under external stimuli such as pH and temperature. UCST type of behaviour was observed for aqueous PAA-PVBTMA-Cl solutions when the hydrophobic trifluoromethanesulfonate (OTf) anion was introduced. In addition, self-assembly of the diblock copolymer was confirmed by zeta potential measurements in different pH conditions. The expected reverse of the micelle structure with changing pH was not observed. However, aqueous PAA-PVBTMA-Cl showed UCST behaviour and micellization induced by the hydrophobic counterion.

Avainsanat – Nyckelord – Keywords
Polyampholytes, stimuli-responsive polymers, hydrophobic counterions

Säilytyspaikka – Förvaringställe – Where deposited

Muita tietoja – Övriga uppgifter – Additional information

TABLE OF CONTENT

ABBREVIATIONS

AA	Acrylic acid
ACPA	4,4’-azobis(4-cyanovaleric acid)
ATRP	Atom transfer radical polymerization
CTA	Chain transfer agent
CTPA	2-(2-carboxyethylsulfanylthiocarbonylsulfanyl)propionic acid
DLS	Dynamic light scattering
DP	Degree of polymerization
IEP	Isoelectric point
LCST	Lower critical solution temperature
LiOTf	Trifluoromethanesulfonic acid lithium salt
NMP	Nitroxide mediated polymerization
NMR	Nuclear magnetic resonance
PISA	Polymerization-induced self-assembly
RAFT	Reversible addition-fragmentation chain transfer
SEC	Size exclusion chromatography
UCST	Upper critical solution temperature
VBTMA-Cl	(Vinyl benzyl)trimethylammonium chloride

1. INTRODUCTION

Polyampholytes are polymers that have both positively and negatively charged repeating units. The charges can be randomly distributed in the polymer chain or the polymer can have a block structure where one block is composed of anionic repeating units and the other of cationic units. Polymers which have both charges in the same repeating unit are called polybetaines.[1] Syntheses of highly ionic block polymers are not straightforward. One popular way is to use a controlled radical polymerization method such as nitroxide mediated polymerization (NMP), atom transfer radical polymerization (ATRP) or reversible addition-fragmentation chain transfer (RAFT) polymerization.[2-4] In RAFT polymerization one utilizes a chain transfer agent (CTA) which leads to simultaneous chain growth. Therefore, polymers have linear conversion-molecular weight profiles with low polydispersities and well-defined chain ends. Furthermore, RAFT polymerization keeps chain ends active and thus, one can continue polymerization by adding more of the monomer. This is the key to successful well-defined block copolymers.[4]

Properties of aqueous polyampholyte solutions are complex owing to the ionic nature of the polymers. Polyampholytes tend to form intra- and intermolecular complexes in salt-free aqueous solutions and therefore, the characterization of polyampholytes, with methods such as size exclusion chromatography (SEC) or titration is not straightforward.[5,6] Furthermore, the solution properties of polyampholytes can be tuned with external stimuli such as temperature or pH. The polyampholytes consisting of weak acid and base form aggregates near isoelectric point (IEP).[1] The change of pH, however, can induce reverse micellization which is the so-called schizophrenic behaviour.[7] Thermoresponsive behaviour can be induced in charged polymers by adding salt or a hydrophobic counterion.[8,9] Responsive polyampholytes have been studied for applications in biomedicine and the fields of catalysis and energy.[10-13]

This thesis consists of a literature part and an experimental part. The literature part describes the theory of polyampholytes and their behaviour in aqueous solutions which deviate from that of neutral polymers. Next, important aspects of RAFT polymerization are introduced. The final part discusses the stimuli-responsive behaviour of polyelectrolytes such as thermoresponsive and schizophrenic behaviour. The experimental part starts with the description of the syntheses of homopolymers poly(acrylic acid) (PAA) and poly[(vinylbenzyl)trimethylammonium chloride] (PVBTMA-Cl) via RAFT polymerization. Then, the use of PAA as a macro-CTA to synthesize PAA-PVBTMA-Cl block copolymer will be described. The analysis of the polymers is discussed in detail. Molar masses of polymers were measured with various methods. Solution

properties of polyampholytes were studied with several methods. The results show that the polyampholyte self-assemble into micelles and show counterion induced upper critical solution temperature (UCST) behaviour.

2. LITERATURE PART

2.1 POLYAMPHOLYTES

Polyelectrolytes are polymers which have either positive or negative charge in repeating units. Typically, polyelectrolytes consist of polymeric backbone and covalently attached charge bearing functional groups creates the charge. Thus, the polyelectrolyte definition is wide, and it includes both synthetic and natural polymers. Polyelectrolyte can be strong or weak depending on the tendency of functional groups to dissociate. Strong polyelectrolytes are fully ionized in the whole pH range, but weak polyelectrolytes are ionized only at a certain pH range.[14,15] Examples of weak and strong polyacids and bases are in Figure 1.

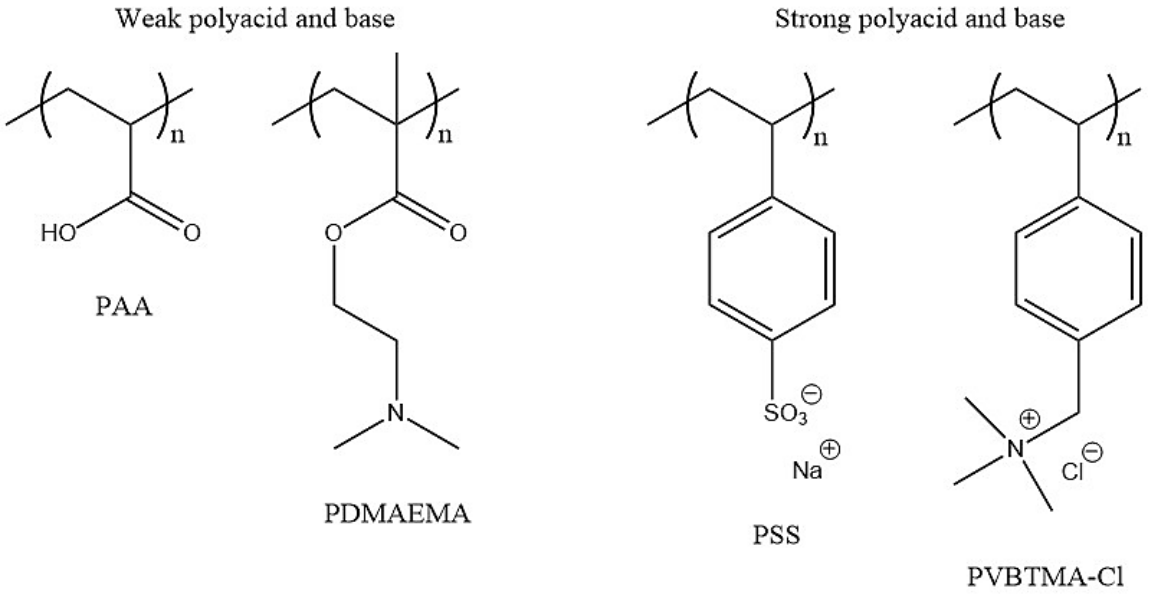

Figure 1. Examples of weak and strong polyacids and bases. From left to right: poly(acrylic acid), poly(2-dimethylaminoethyl methacrylate), poly(sodium 4-styrenesulfonate) and poly[(vinylbenzyl)-trimethyl-ammonium chloride].

Polyampholyte is a polyelectrolyte which has both positively and negatively charged groups. They are also called as polyzwitterions and polybetaines depending on the location of the charges in the polymer chain.[1,16,17] Here, the polyampholytes refers to polymers that have cationic and anionic groups on different monomer units. The polyzwitterions and polybetaines, on the other hand, refer to the polymers, which have cationic and anionic groups on the same monomer unit. Examples of polyampholyte and polyzwitterion are in Figure 2.

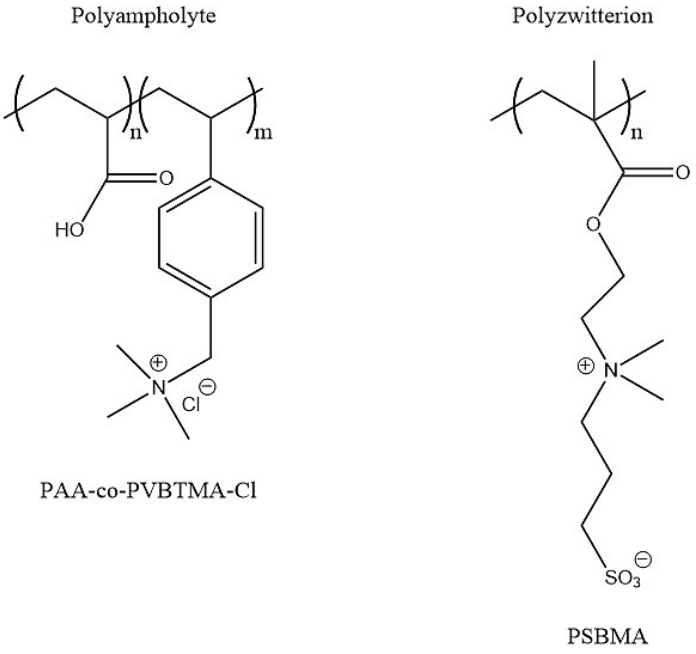

Figure 2. Examples of polyampholyte, poly(acrylic acid)-co-poly[(vinyl-benzyl)trimethylammonium chloride] (left), and polyzwitterion, poly[*N*-(3-sulfopropyl)-*N*-methacryloxyethyl-*N*,*N*-dimethylammonium betaine] (right).

Copolymer consists of different monomer repeating units, therefore, various structures are possible such as alternating[17], block[18-20], statistical[21] (also known as random), and graft[22,23]. These different structures of a copolymer are illustrated in Figure 3. There are different synthetic methods to produce controlled ampholytic polymers and with different copolymer structures. In alternating structure, every monomer unit of A is altered by another monomer unit B. Saha *et al.*[17] synthesized poly(styrene-alt-maleimide) alternating polyampholyte by using *N*-maleoyl-L-leucine *tert*-butyl ester with a *tert*-butyl carbamate (Boc)-protected leucine appended styrenic monomer via RAFT polymerization. Block copolymers, which consist of different homopolymer chains covalently bonded to each other, can be polymerized by using

controlled radical polymerization methods.[2,3,24] In statistical structure, all monomer units are polymerized randomly and therefore only kinetics of polymerization affects polymer composition. Graft polymers consist of two different types of polymers or substrates. These polymers can be synthesized with “grafting from” or “grafting to” -methods. In the grafting from -method, the active site of polymeric backbone or substrate is used to polymerize new polymer branch with different monomers. In the grafting to -method, the ready polymer chain is attached to the active site of polymeric backbone or substrate by chemical reaction.[22,23,25]

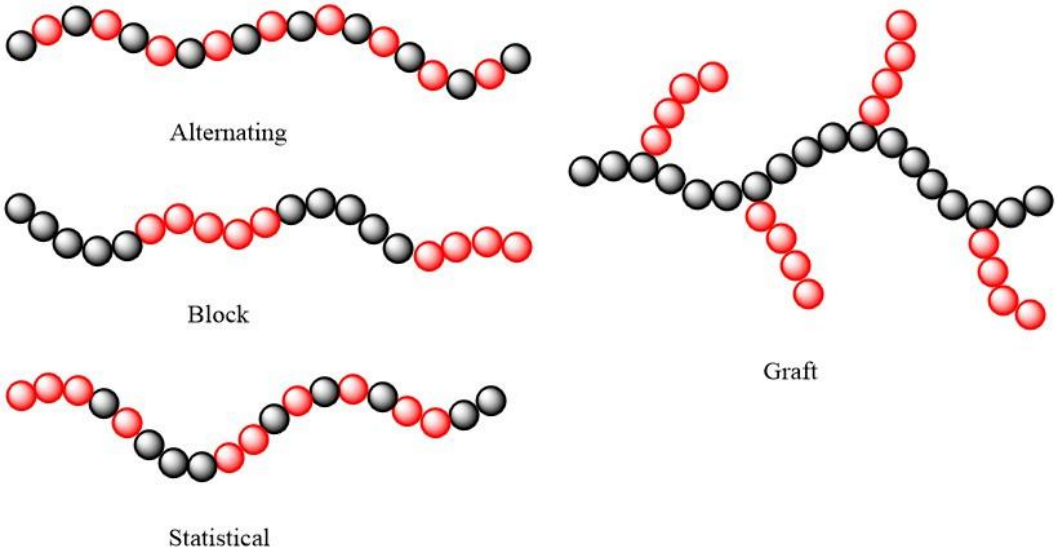

Figure 3. Different structures of the copolymer.

In addition to different structures, polyampholytes and polyelectrolytes can have different sort of architectures such as linear, branched[26,27], star-shaped[22,28] or dendrimer[29] and these are illustrated in Figure 4. The linear architecture is the simplest one and block copolymers even with 20 blocks have been synthesized.[30,31] Star-shaped copolymers can be synthesized by using “core first” or “arm first” -methods. In the core first approach, the core of the star is synthesized first and then arms are synthesized on the core. In the arms first approach, the arms are synthesized first and then reacted with a core. Star-shaped copolymers can have a block structure in arms, or the star-shaped polymer can consist of different homopolymer arms.[28] Dendrimeric polymers are also possible to synthesize, for example, poly(propyleneimine) dendrimers with a carboxylate end groups have been made.[29]

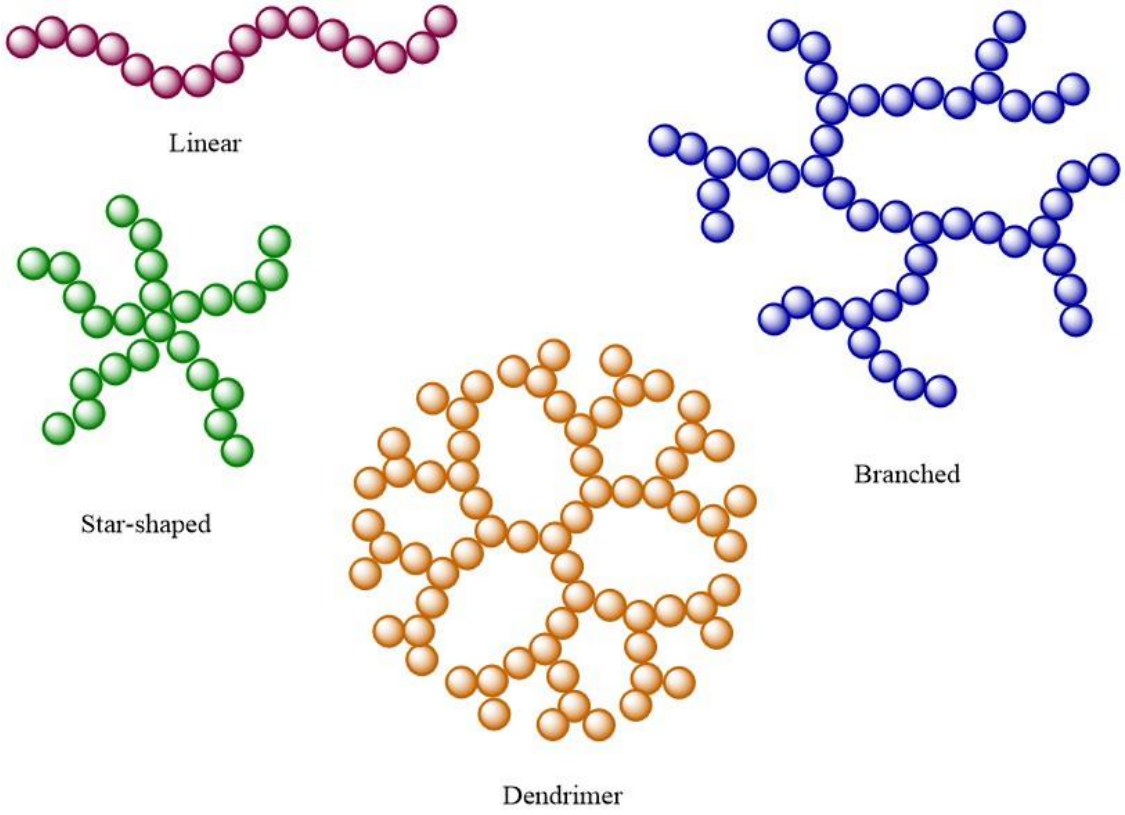

Figure 4. Different architectures of polymers.

The polyampholytes have strong Coulombic interactions which can lead to branched architecture. The branched structure is formed by ionic cross-linking due to attraction between anionic and cationic groups. Random branching creates a three-dimensional polymeric network, which is called a gel. The addition of small molecular salt affects gel formation due to screening of functional group charges and the formation of ion pairs between functional groups and salt ions.[27] The branched structure can also form because the monomers tend to react themselves. Acrylic acid is this sort of monomer and it is known to form dimers spontaneously by Michael-type addition upon standing even if inhibitors are present. Therefore, synthesis of acrylic acid can produce branched structure due to dimers especially if monomer solution is heated. Another feature which can accelerate dimerization of acrylic acid is deoxygenation. [32]

2.2 SOLUTION PROPERTIES

2.2.1 EFFECTIVE CHARGE

Compared to non-charged polymers, polyelectrolytes and polyampholytes behave very differently, especially in solutions. Weak and strong polyelectrolytes tend to dissociate in aqueous solutions and form charged polymer chains. Polyelectrolytes, however, have different properties compared to small molecular salt. One important difference is related to the dissociation of functional groups. Small molecular salt dissolves molecularly and time needed to stabilize the solution is short. However, the polyelectrolyte system is more complex, and the ionization of weak polyelectrolyte can be divided into three different stages. The first stage is the complete dissociation, where the counterion has detached from the functional group and hence, has no interactions with the polymer and its free to move in the solution. The second stage is intermediate dissociation, where counterions are dissociated from functional groups but are still in the electric field of a polymer. Therefore, counterions have interactions with charged polymer and are not completely free to move in solution. This is called ion binding. The final stage is condensed counterions which are bonded functional groups of the polymer. These different ionization stages are illustrated in Figure 5.[33]

Due to different ionization stages polyelectrolyte is characterized by effective charge. An effective charge is a charge which polymer has in use, and it differs from a number of functional groups due to condensed counterions and ion binding. However, there are different theoretical models which describe ionization of polyelectrolytes and depending on the model the terms describing ionization varies.[6,34,35] Terms ion binding and counterion condensation are often used in theoretical models which divides counterions to bound and free ones and the term counterion distribution is often used in the mean-field approximation model.[35,36] These theoretical models are described in more detail in the next chapter.

Dissociation of polyelectrolytes is a complex process and therefore counterions can be described with an activity. Activity describes the number of free counterions, and it can be used to get information about the effective charge or ion binding indirectly. Activity is used to describe the non-ideal chemical systems such as polyelectrolyte solutions where ions are not only bound or free but there is also ion binding in the system. In addition, different solution parameters affect counterion activity such as ionic strength, polyelectrolyte concentration and charge of polyelectrolyte.[37]

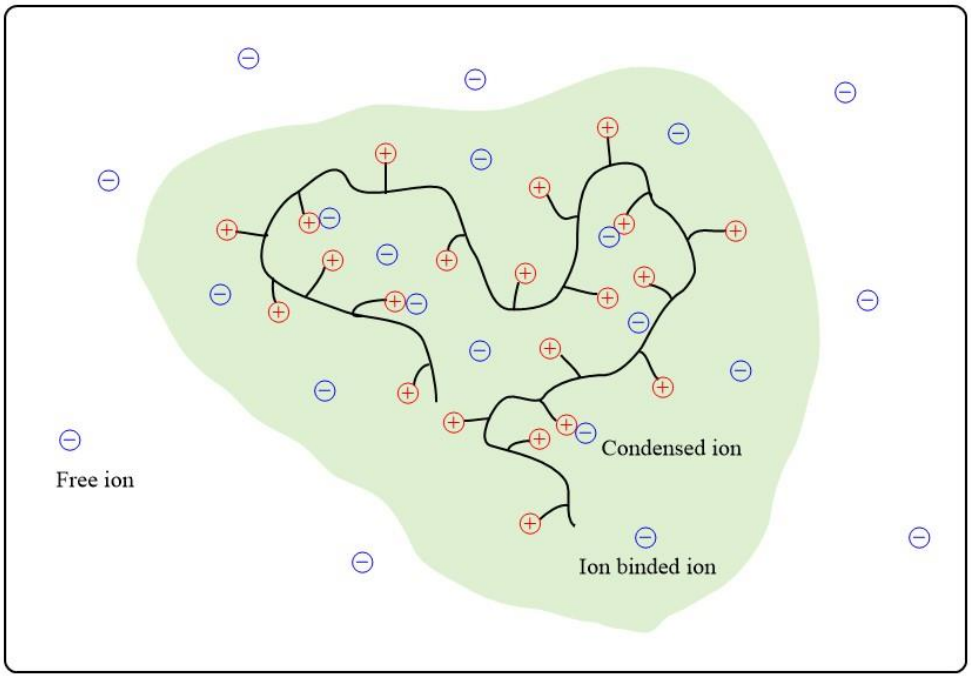

Figure 5. Illustration of different dissociation stages of weak polyelectrolyte. Green area represents electrostatic interactions of polyelectrolyte and non-condensed counterions inside the green area are ion bonded.

2.2.2 TITRATION OF POLYMERS

Polyelectrolytes can be divided for two groups according to their acid-base properties. Strong polyelectrolytes are comparable to strong acids and bases which fully ionizes without dependence of pH. Weak polyelectrolytes are comparable to weak acids and bases whose ionization depends much on solution conditions and pH. However, there is a fundamental difference between small molecular acids and bases compared to polyelectrolytes due to a large number of ionizable groups. Titration curves of polyelectrolytes can contain large buffer region and change in the titration curve can be gradual. Therefore, it is difficult to determine the equivalence point or pK_a value for polyelectrolytes. Due to the complexity of titration curve analysis, Oosawa-Manning condensation theory, the mean-field approximations and site binding model were developed to describe dissociation of polyelectrolytes.[6,38-40]

In the Oosawa-Manning condensation theory, the counterions are divided into condensed or free and the third option (ion binding) is neglected. The free counterions can move in whole solution volume V except in polyelectrolyte region and, condensed counterions can move only small volume surrounding polymer backbone. Furthermore, the polymer backbone is studied

as a linear rod which contains charges and it does not take into account the flexibility of chains. In Figure 6A is an illustration of Oosawa-Manning condensation theory where condensed counterions can move only near polyelectrolyte's charges which are presented as a cylindrical region around polyelectrolyte. The free counterions can move only outside of cylinder accordingly. The main limitation of Oosawa-Manning condensation theory is that it is oversimplified of a real situation where ions can have interactions without condensation and polymer backbone can change conformation.[35,41]

Compared to the Oosawa-Manning condensation theory, the mean-field approximations (also known as Katchalsky's cell model) is a more exact model describing counterion distribution around polyelectrolyte. The mean-field approximations are based on solving the non-linear Poisson-Boltzmann equation which can be achieved analytically only for rod-like polyelectrolytes and planar charged surfaces. The Poisson-Boltzmann equation describes the distribution of electrostatic potential around polyelectrolyte and therefore the distribution of counterions around polymer is obtained. When the distance from charged polyelectrolyte increases, the electrochemical potential decreases and therefore counterion density decreases and this is illustrated in Figure 6B. In the mean-field approximation, it is also possible to use other Poisson-Boltzmann equation such as Debye-Hückel theory. The limitation in the mean-field approximation is that counterions are not considered as particles but with charge density and solvent molecules are considered as continuous media and not as molecules.[35,42]

Site binding model is an expansion for the Ising model which is developed for magnets. In the site binding model, every ionizable functional group is considered individually and each ionizable group is numbered from 1 to N. Each functional group can be protonated (s_i=1) or non-protonated (s_i=0). Thus, these individual groups are defined by their microstate. Every microstate has its own pK_i value. In addition, the interaction parameter (ε) is considered due to the electrostatic interactions of charged groups. The protonation of the whole polyelectrolyte is calculated from the sum of free energy of individual microstates and all the possible configurations which gives free energy of the whole polymer. Therefore, equation (1) can be used to determine the free energy of polymer,

$$\frac{\beta F(s_1,s_2,\ldots s_N)}{\ln 10} = -\sum_i pK_i s_i + \sum_{i>j} \varepsilon_{ij} s_i s_j \qquad (1)$$

where $1/\beta = kT$ (k is Boltzman's constant and T is absolute temperature) and ε_{ij} is an interaction parameter between sites i and j. Equation (2) gives the relation between free energy and activity of H^+ ions and therefore for pH:

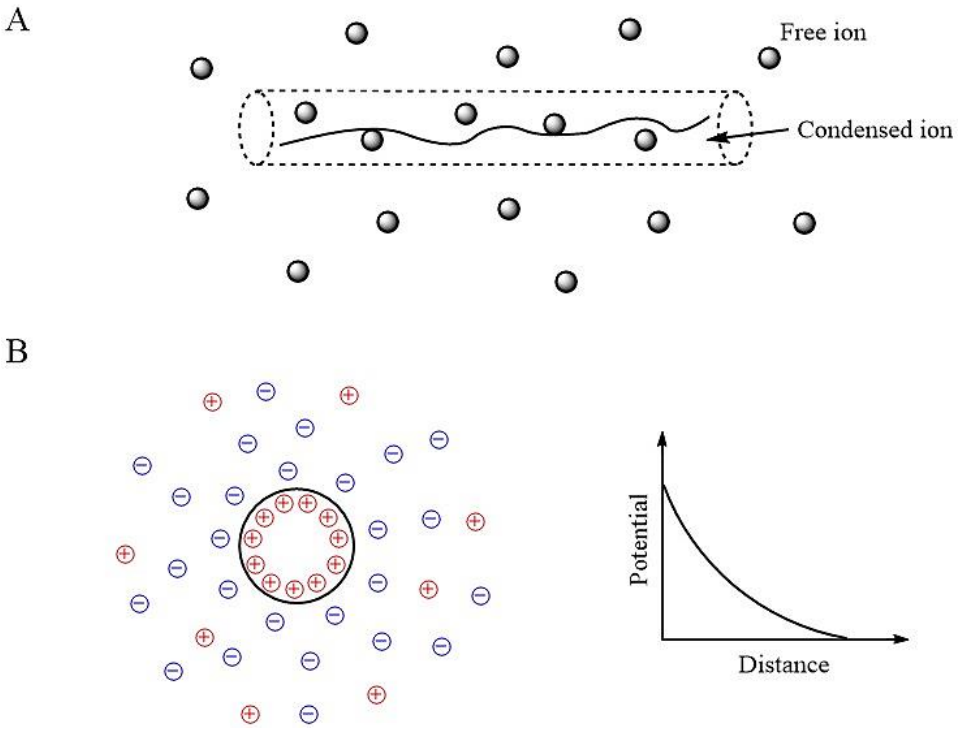

Figure 6. Illustration of counterions of polyelectrolyte according to a) Oosawa-Manning theory and b) the mean-field approximation model (when the distance from charged surface increases, electrochemical potential decreases).

$$\Xi = \sum_{s_i,\dots s_N} a_H^n e^{-\beta F(s_1,s_2,\dots s_N)} = \sum_{n=0}^{N} \bar{K}_n a_H^n \tag{2}$$

The last part of the equation (2) is achieved by grouping terms together as equation (3) implies:

$$p\bar{K}_n = \lg \frac{\bar{K}_n}{\bar{K}_{n-1}} \tag{3}$$

The protonation θ is given by the derivative in equation (4):

$$\theta = \frac{a_H}{N} \frac{\partial \ln \Xi}{\partial a_H} \tag{4}$$

Site binding model can be used in different ways. The simplest model assumes that all ionizable groups have same pK_i value and only nearest group interactions are taken into account. However, the more realistic model considers long-range interactions and whether the ionizable group is primary secondary or tertiary. In addition, different sort of interactions can be considered. For linear polyelectrolyte small plateau is observed when interactions are considered. The main reason is that half of the polyelectrolyte is then protonated and an increasing number of charges needs more energy due to electrostatic repulsion in homopolymer.[6]

2.2.3 POLYELECTROLYTE AND ANTI-POLYELECTROLYTE EFFECT

Dissociation of polyelectrolyte salt makes polymer charged. Charges are localized in a relatively small space in the polymeric backbone, leading strong electrostatic interactions into the polymer. In homopolyelectrolytes, all functional groups have like charges and thus the repeating units repel each other. Therefore, Coulombic interactions make the polymer to elongate. Elongated polymers cannot move as freely as coiled polymers due to larger dimension and higher friction caused by charged chains. Therefore, solution viscosity increases when the degree of ionization increases. Furthermore, dilution of polyelectrolyte solution increases viscosity number because more ionization is taking place. Dilution also reduces interchain interactions which affect viscosity.[36,43,44] This phenomenon is called polyelectrolyte effect and it is illustrated in Figure 7. For example, dialysis of polyelectrolyte dilutes polymer solution which increases viscosity number. Polyelectrolyte effect can be affected by adding small molecular salt. Small salt molecules screen the charges of functional groups which decreases elongation of a polymer. Therefore, charged polyelectrolyte changes its conformation back to coiled one and start to behave as neutral polymer.[43,44]

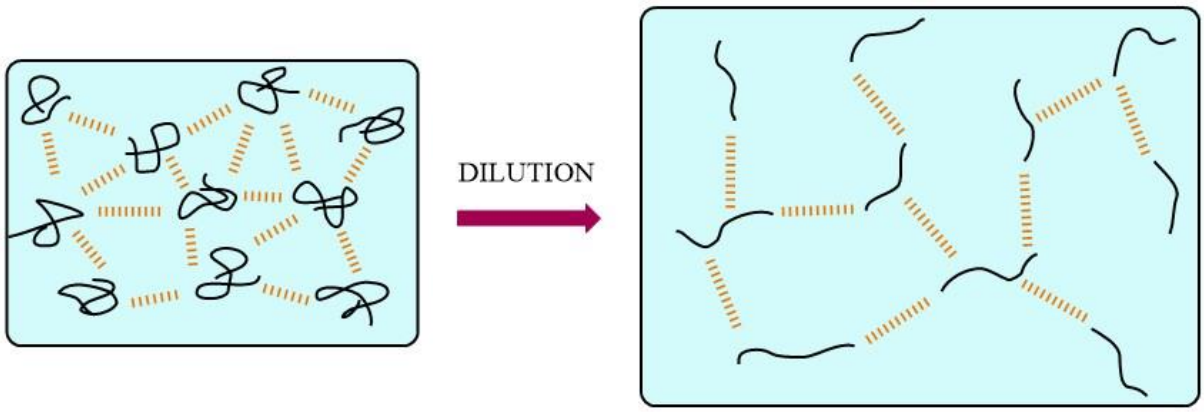

Figure 7. Illustration of polyelectrolyte effect. Black curves represent polymers and dashed lines represent interactions between polymers. Dilution decreases interactions between polymers and increases charge density which leads to more elongated conformation and higher viscosity.

Even though the polyelectrolyte effect is important for charged polymers, the situation is more complicated in the case of polyampholytes and polybetaines due to cationic and anionic groups. Polyampholytes have an isoelectric point, which is the pH where polyampholytes form a neutral polymer. In the IEP dissociation of cationic and anionic groups leads both intra- and

intermolecular interactions which cause polyampholyte to collapse to a globular conformation. However, the addition of small molecular salt will screen the charges of functional groups, leading the expansion of globule to coil conformation and this is called the anti-polyelectrolyte effect. The anti-polyelectrolyte effect is seen as a smaller particle size and reduced solution viscosity near the IEP and viscosity and particle size will increase with an increasing amount of small molecular salt. However, the anti-polyelectrolyte effect is dependent on polyampholyte composition and polyampholytes which have a large net charge does not have the anti-polyelectrolyte effect but polyelectrolyte effect.[1,16,45,46]

2.2.4 OSMOTIC PRESSURE AND DONNAN POTENTIAL

Important features for polyelectrolytes are osmotic pressure and Donnan potential. According to IUPAC[47] osmotic pressure is "excess pressure required to maintain osmotic equilibrium between a solution and pure solvent separated by a membrane permeable only to the solvent". Thus, the system needs a solution and pure solvent on different sides of the semipermeable membrane which creates an electrochemical potential difference. However, the membrane does not allow polyelectrolyte or counterions to go through the membrane to stabilize electrochemical potential. Therefore, a pure solvent is flowing through the membrane to the concentrated solution and creates a pressure gradient. This pressure gradient stabilizes electrochemical potential in the system and forms osmotic equilibrium (see Figure 8).[48,49]

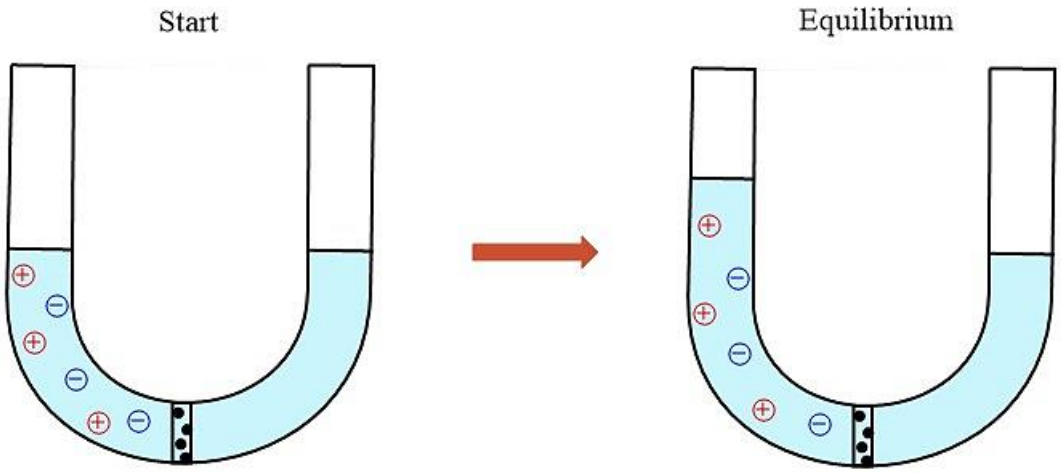

Figure 8. Illustration of osmotic pressure.

In Donnan potential, polyelectrolyte solution which contains small molecular salt is separated from the pure solvent with a semipermeable membrane that allows small molecules to go through the membrane. Therefore, an electrochemical potential difference between the polymer solution and pure solvent drives small molecular salt through the membrane. After equilibrium is reached electroneutrality remains. However, polyelectrolyte cannot go through the membrane which leads to an uneven number of small molecular salt on different sides of the membrane. If polyelectrolyte has a positive charge, there is an uneven number of small molecular cations on different sides of the membrane. This leads to the potential difference across the membrane which is called Donnan potential and it is compensated with a pressure term called colloid osmotic pressure.[47,50,51] Corresponding equilibrium state is called Donnan equilibrium.[47,51] Donnan potential formation is illustrated in Figure 9. In addition, Donnan potential is formed in more complex systems where polymers are both sides of membrane.[51]

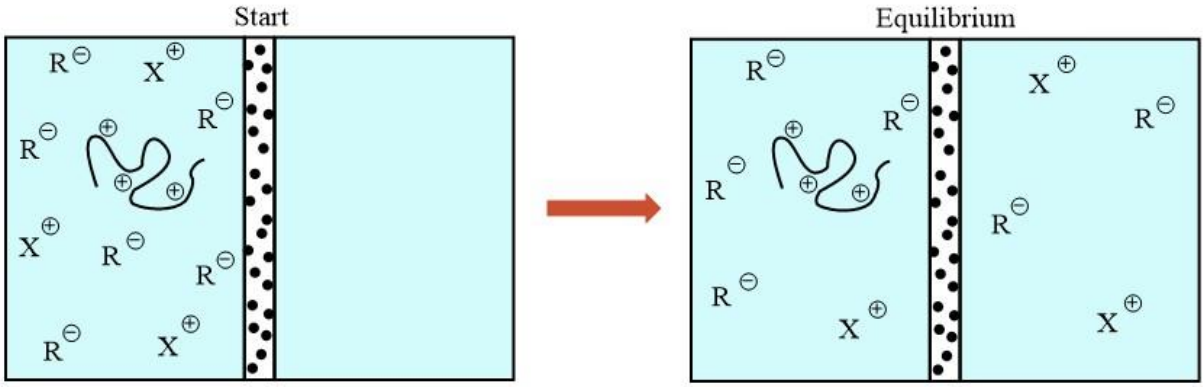

Figure 9. Illustration of Donnan potential. Small salt molecules diffuse through the semipermeable membrane to stabilize electrochemical potential difference. In equilibrium, there is an uneven number of cations on a different side of the membrane which causes Donnan potential.

Donnan potential and osmotic pressure have a tremendous effect in practical applications. One good example is the purification of polyelectrolyte by dialysis. In dialysis, a polyelectrolyte solution is purified with a semipermeable membrane tube. The membrane allows small molecules and water to go through but leaves polymer inside the tube. Thus, impurities and unreacted monomers can be removed from the polyelectrolyte solution. If polyelectrolyte is purified with pure solvent, counterions are also partially removed from the polymer solution. This causes elongation of polymers and increasing viscosity according to the polyelectrolyte effect. In addition, charged polyelectrolyte causes Donnan potential to a system that is

compensated with osmotic pressure and solvent flows to polyelectrolyte solution. Therefore, the dialysis tube swells a lot during the purification process until the system reaches equilibrium.

2.3. RAFT POLYMERIZATION

2.3.1 CONTROLLED RADICAL POLYMERIZATION

There are three controlled radical polymerization methods: NMP[2,52,53], ATRP[3,54,55] and RAFT polymerization[24,56,57]. In all previously mentioned methods, there is an equilibrium between propagating (active) and dormant (non-propagating) states of polymer chains. NMP and ATRP are based on reversible deactivation of propagating chains whereas RAFT polymerization is based on degenerative chain transfer and therefore in RAFT polymerization radicals must be produced with an initiator.[24] In all previously mentioned polymerization methods, the number of active chains is kept low and therefore, polymers grow simultaneously. Controlled polymerization leads to linear conversion-molecular weight profile and low polydispersity.[2,55,57] RAFT polymerization produces well-controlled end groups that can be used in the characterization of a polymer.[24] In addition, RAFT polymerization is a popular method to synthesize polyelectrolytes due to stability towards charged monomers.[9,18,58] In further discussion, RAFT polymerization is described in more detail.

2.3.2 RAFT POLYMERIZATION MECHANISM

RAFT polymerization starts as free radical polymerization. Initiator reacts with a monomer and creates a radical species which can then propagate. The propagating chain then reacts with CTA which either release the original growing chain or releases an active group R which can initiate a new growing chain. This step is called fragmentation. However, it is possible that the initiator reacts directly with CTA without the addition of any monomer. After all free CTA is consumed polymerization reaches an equilibrium where polymers switch reversibly between active and dormant states. CTA keeps the number of active radicals low and suppresses termination reactions. However, in all radical polymerization methods, termination reactions are always present. In Scheme 1 is illustrated the RAFT polymerization mechanism.[57]

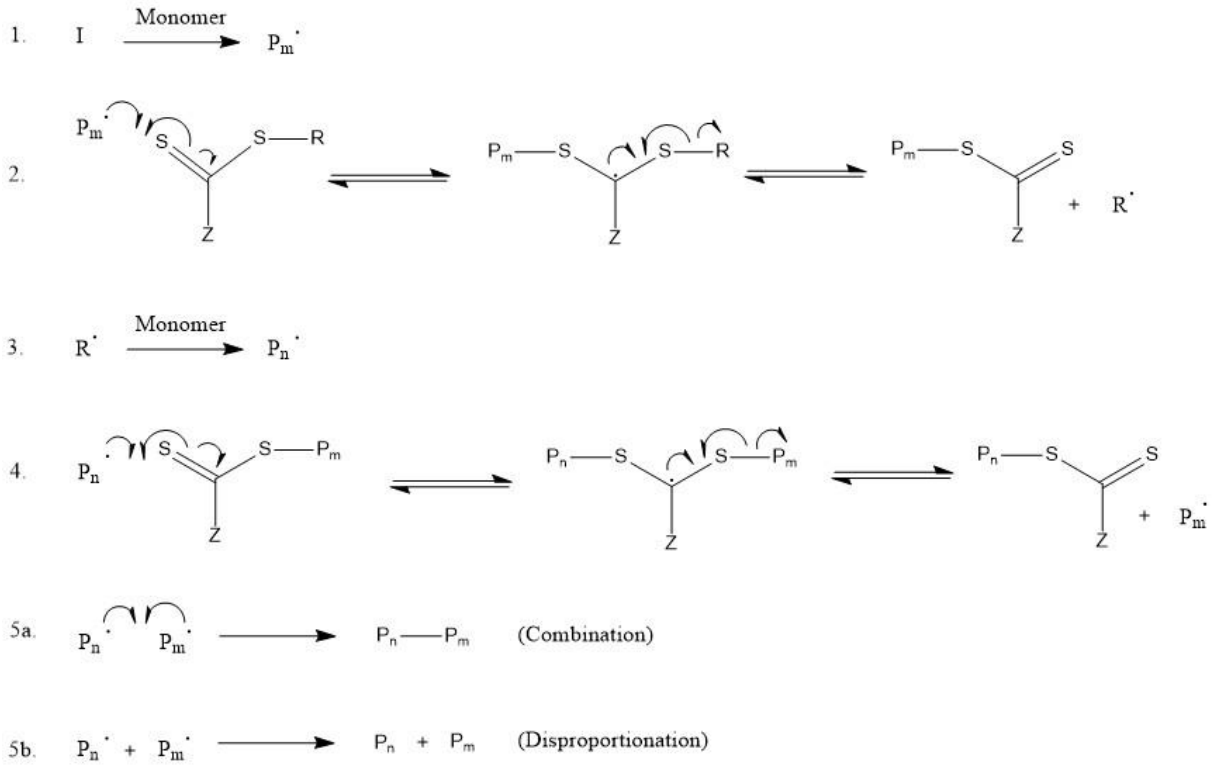

Scheme 1. Illustration of RAFT polymerization.

In RAFT polymerization the most of polymer chains are initiated by CTA and therefore the amount of initiator does not affect the number of chains. If it is assumed that polymer chains are only initiated by CTA and termination reactions are negligible, theoretical degree of polymerization ($DP_{theor.}$) can be calculated from equation (5).

$$DP_{theor.} = \frac{[M]_0}{[CTA]_0} \times \text{conversion} \quad (5)$$

In equation (5) square brackets are initial concentrations and conversion is the number of reacted monomers. Therefore, equation (5) presents the total number of reacted monomers divided by the number of chains. When the molecular weight of monomer and CTA is known, the theoretical molar mass of the polymer ($M_{n,theor.}$) can be calculated from equation (6).

$$M_{n,\ theor.} = DP_{theor.} \times M(M) + M(CTA) \quad (6)$$

In equation (6) *M(M)* is the molecular weight of monomer and *M(CTA)* is the molecular weight of CTA. When equations (5) and (6) are combined, equation (7) is obtained.

$$M_{n,\ theor.} = \frac{[M]_0}{[CTA]_0} \times conversion \times M(M) + M(CTA) \quad (7)$$

With equation (7) it is possible to calculate the theoretical number average molar mass with initial concentrations and conversion.[24]

2.3.3 CHAIN END ACTIVITY

Even though an initiator does not affect a number of growing chains it affects termination reactions and the fraction of "living" chains meaning that chain ends stay active. Thus, the number of termination reactions can be controlled by the number of radicals introduced in the system and therefore with the amount of initiator. When the amount of initiator is decreased, termination reactions are suppressed which leads to higher "livingness". The livingness of the polymer chain can be calculated from equation (8)

$$L = \frac{[CTA]_0}{[CTA]_0 + 2f[I]_0\left(1 - e^{-k_d t}\right)\left(1 - \frac{f_c}{2}\right)} \quad (8)$$

where L is the livingness, $[CTA]_0$ and $[I]_0$ are the initial concentration of CTA and initiator respectively, f is the initiator efficiency and k_d is the decomposition rate of the initiator. The term "2" before f means that the initiator produces two radicals and the term $1-f_c/2$ represents the number of dead chains (when $f_c = 1$, 100% bimolecular termination is by combination; when $f_c = 0$, 100% bimolecular termination is by disproportionation).[24,59] High chain end activity is important especially when block polymers are synthesized to get block polymers with high yield. Even polymers with 20 blocks are synthesized with RAFT polymerization with good control of molar mass.[59]

2.4 SELF-ASSEMBLY OF COPOLYMERS

Block copolymer self-assembly was traditionally accomplished by changing the solution conditions. First, the copolymer was dissolved in a suitable solvent for both blocks, then the copolymer solution was transferred to the non-suitable solvent for one of the blocks. The more insoluble block formed a core and the more soluble formed corona in self-assembled structures.[60] The copolymers can self-assemble into different morphologies such as spherical micelles, cylindrical or worm-like micelles, lamellae, vesicles or schizophrenic micelles.[58,60,61]

Different morphologies are illustrated in Figure 10. However, nowadays there are various functional polymers that can self-assemble without any solvent exchange. For instance, changing the external stimuli can induce self-assembly into nanostructures.[62-64] The self-assembly of copolymers can also be achieved by changing the counterions in the aqueous conditions.[65] A recent synthetic approach, polymerization-induced self-assembly (PISA), has also been employed to form self-assembled nanoparticles from various copolymers.[58]

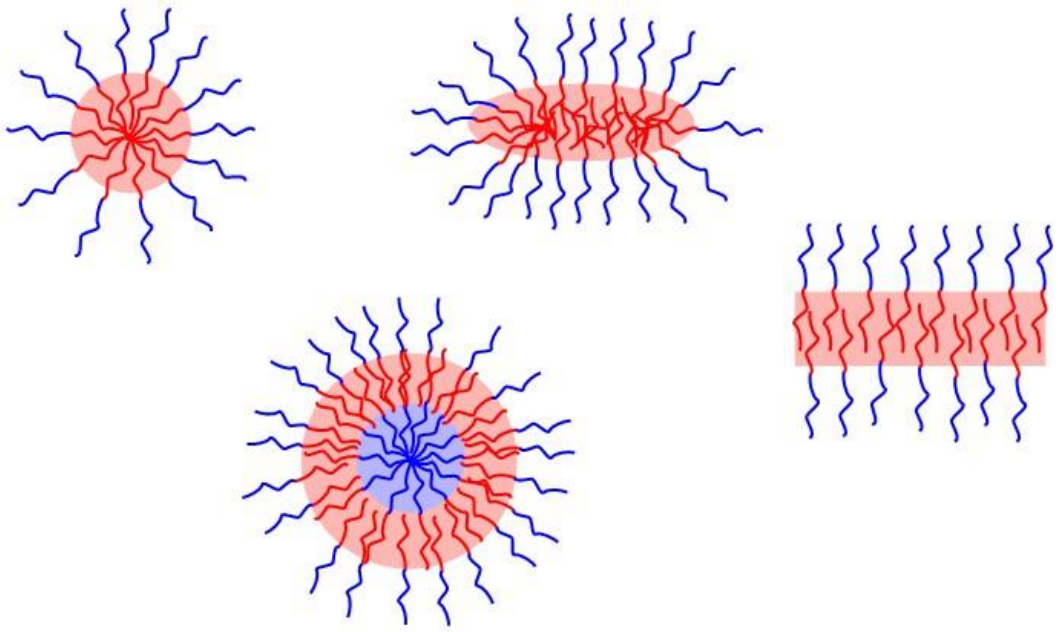

Figure 10. Self-assembly morphologies of block copolymers. From left to right: spherical micelle, vesicle, rod-like micelle and lamella.

The morphology of block copolymer depends on the packing parameter (*P*). The packing parameter is defined with equation (9),

$$P = \frac{v}{a_0 l_c} \tag{9}$$

where v is the volume of hydrophobic chains, a_0 is the optimal area of head group and l_c is the length of the hydrophobic tail.[66] Thus, the amount of more hydrophobic block has an important effect on polymer conformation. With the packing parameter, it is possible to predict the conformation of a block copolymer; spherical micelles are preferred when $P \leq 1/3$, cylindrical micelles when $1/3 < P \leq 1/2$ and vesicles when $1/2 < P \leq 1$. However, these predictions are only directive and very complex morphologies have been accomplished such as jellyfishes or oligolamellar vesicles.[58]

2.5 SCHIZOPHRENIC POLYMERS

Schizophrenic block copolymers have a unique property to self-assemble in water solutions without any organic solvent.[67] However, schizophrenic micelles differ from "normal" micelles due to stimuli-responsive behaviour. Schizophrenic polymers undergo reversible micellization from the core to corona or vice versa when the solution conditions are changed.[67] Therefore, schizophrenic polymers can respond to external stimuli such as pH[19,68], salt[64] or temperature[69,70] and this is illustrated in Figure 11. Schizophrenic polymers can have conditions where both blocks are dissolved as unimers, and therefore, micelle structure is not formed in those conditions.

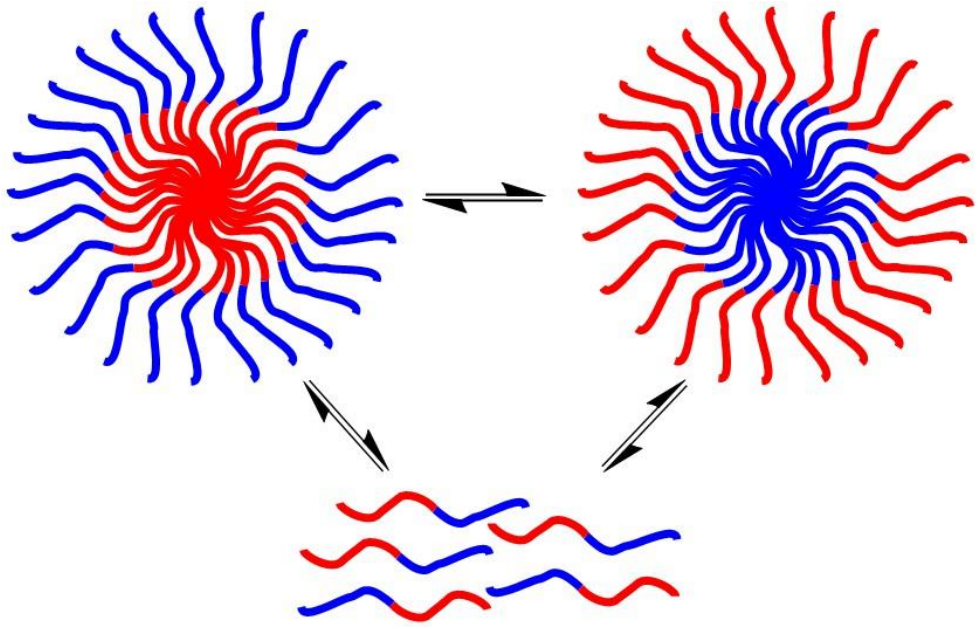

Figure 11. Illustration of self-assembly of a block copolymer. Red and blue parts represent different blocks in a copolymer and when solution conditions are changed core and corona changes vice versa. Schizophrenic polymers can have a condition where both blocks are dissolved as unimers which is illustrated with single chains.

For example, a copolymer which has a block containing secondary amines and a block containing carboxylic acids is double pH-responsive. In acidic conditions, the carboxylic acid is neutral, and amine has a positive charge and therefore carboxylic acid forms the core of micelle and amine forms the corona due to better solubility of amine. When conditions are changed to basic, carboxylic acid gets a negative charge and forms the corona of the micelles.

However, it is not necessary to have both blocks reacting to the same stimulus. For example, combinations pH plus temperature[71] or pH plus salt[67] are possible. In addition, the copolymer can consist of more than two blocks which make the system even more complex.

Even though schizophrenic block copolymers can have many different stimuli-responses there are some limitations in polymer architecture. Block copolymer must be quite symmetric to produce stable micelles. When the first block is much larger than the second block it is difficult to stabilize micellar structure where a large block is in the core. In addition, asymmetric block copolymers can result in more polydisperse micelles.[67] Thus, careful selection of the block ratio is needed to produce stable schizophrenic micelles.

2.6 THERMORESPONSIVE POLYMERS

Thermoresponsive polymers belong to the class of stimuli-responsive materials. Thermoresponsive polymers are divided to lower critical solution temperature (LCST) and upper critical solution temperature type of polymers according to the temperature-dependent phase transition as illustrated in Figure 12. The LCST type of polymers are soluble below the critical solution temperature, but they phase separate upon increasing the temperature above the LCST. The UCST behaviour is opposite to LCST, these polymers are insoluble below the critical solution temperature but they become soluble by increasing the temperature above UCST.[47,72] The well-known thermoresponsive polymer is poly(*N*-isopropylacrylamide) pNIPAM exhibiting LCST type of behaviour.[73] UCST type of behaviour is known for example for polysulfobetaines and poly(*N*-acrylolyglycinamide) [poly(NAGA)].[74-76]

Even though polyelectrolytes can have thermoresponsive behaviour themselves, thermoresponsive behaviour can be induced with a careful selection of counterion. For example, Karjalainen *et al*.[9] have shown that hydrophobic anion such as OTf or NTf_2 can induce UCST type of behaviour in polycation solutions. However, the amount of hydrophobic anion and ionic strength must be high enough to screen intra- and intermolecular electrostatic interactions in order to induce the thermoresponsive behaviour.

Baddam *et al*.[77] have shown that the block ratio of a cationic block in poly(ethylene glycol)-*b*-poly(vinylbenzyl trimethylammonium triflate), PEG-PVBTMA-OTf, affects the thermoresponsive behaviour. When the cationic block was shorter, phase separation happened in different stages; first, the polymer phase-separated during cooling but started to mix again

with further cooling. However, with longer cationic block phase separation happened in one step. Sharker *et al.*[78] who have studied P(VBTAC/NaSS) statistical polymer, which is strong polyampholyte, have shown that molar mass of polymer, polymer concentration and salt concentration affect UCST of the polymer. When molar mass and polymer concentration increases also UCST increases and when salt concentration increases UCST decreases. Therefore, phase transition temperature can be adjusted with a molar mass of polymer and solution conditions.

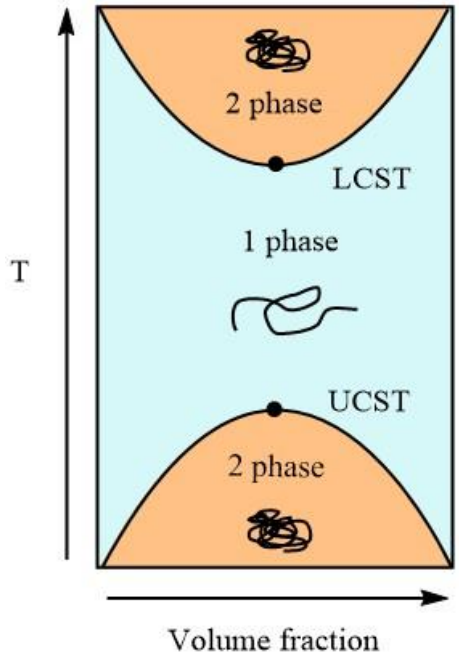

Figure 12. Schematic presentation of LCST and UCST type of behaviour.

AIM AND OBJECTIVES OF THIS STUDY

The aim of this study was to synthesize and characterize ampholytic block copolymer which consists of weakly charged anionic (PAA) and strong cationic (PVBTMA-Cl) blocks. Syntheses of polyampholyte were conducted via RAFT polymerization using PAA as a macro-CTA. In addition, homopolymer PVBTMA-Cl was prepared to compare its properties with the polyampholyte. The second aim of this work was to study the solution properties of the polyampholyte. Polyampholytes which consist of a weak acid and base units have shown schizophrenic behaviour with a change of pH.[63] In addition, PEG-PVBTMA-OTf and PVBTMA-OTf have shown UCST type of thermoresponsive behaviour induced by the hydrophobic counterion.[18] Therefore, in this thesis, the polyampholyte was studied in solutions with added hydrophobic salt and as a function of pH to characterize stimuli-responsive behaviour.

The chosen topic was difficult because of the high number of factors affecting the polymer properties. However, the subject is very interesting for the master's thesis. Due to strong electrostatic interactions typical for polyampholytes, synthesis conditions needed to be carefully optimized. In addition, several characterization methods were used to obtain molar masses of polymers. Finally, the sensitivity of the polyampholyte to stimuli like temperature and pH was studied with several methods. Owing to the strong inter- and intramolecular interactions in the polymers the molecular characterization was tedious, however, it was possible to draw a general picture of the solution behaviour of the polymer.

3. EXPERIMENTAL PART

3.1. MATERIALS

(Vinylbenzyl)trimethylammonium chloride [(VBTMA)Cl; 99%], acrylic acid (AA; 99%) and 2-(2-carboxyethylsulfanylthiocarbonylsulfanyl)propionic acid (CTPA; 95%) were used as received from Sigma. 4,4'-azobis(4-cyanovaleric acid) (ACPA; ≥75%) was recrystallized from methanol. Trifluoromethanesulfonic acid lithium salt (LiOTf; 99.995%, Sigma), diethyl ether (J. T. Baker), 1,4-dioxane (Fischer Scientific) sodium hydroxide pellets (NaOH; 98.5 – 100.5%, VWR chemicals) and hydrochloric acid (HCl; ≥37%, Honeywell) were used as received. Deionized water was purified with ELGA purelab ultrapurification system and was used in all experiments. The regenerated cellulose tubes (from Spectrum) with a molecular weight cut off 1000 $gmol^{-1}$ and 6000–8000 $gmol^{-1}$ were used for the dialysis process.

3.2. SYNTHESES

3.2.1 SYNTHESIS OF POLYACRYLIC ACID

Polyacrylic acid was synthesized via RAFT polymerization by using CTPA as a chain transfer agent. In Figure 13 is the schematic illustration of PAA synthesis. The synthesis of PAA was as follows: the monomer, AA (5.00 g, 69 mmol), CTPA (0.35 mg, 1.4 mmol) and dioxane (15 mL) were added into 50 mL two-necked round-bottomed flask. The initiator, ACPA (77.76 mg, 0.28 mmol) was dissolved in dioxane (5 mL) in a separate vial. The two solutions were purged with argon about 15 minutes before transferred to the same reaction flask. Purging was continued for 25 minutes, then the reaction flask was transferred in an oil bath heated to 70 °C.

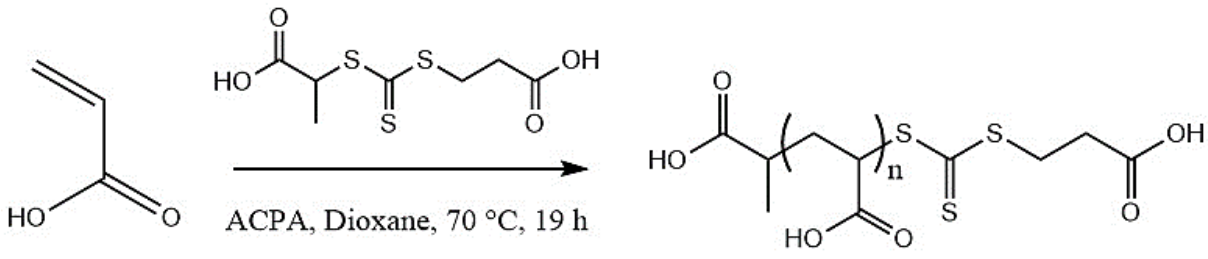

Figure 13. Synthesis of PAA macro-CTA via RAFT polymerization.

Conversion sample was taken after 17 h reaction time and was analysed with ^{1}H NMR in D_2O and dimethyl sulfoxide-d_6 (DMSO-d_6). The conversion of monomers was 90% from the NMR and therefore polymerization was ended after 19 h reaction time. The crude PAA homopolymer was purified by precipitation to cold ether. However, some dioxane was left in the precipitate and with time polymer dissolved again. Therefore, the polymer was further purified by dialysis against water for three days and then collected the polymer by freeze-drying the dialyzed solution. The MWCO 1000 $gmol^{-1}$ dialysis tubes were used for the purification. The yield of the reaction was 3.37 g. The purified PAA homopolymer was further used as a macro-CTA to obtain PAA-PVBTMA-Cl block copolymer.

3.2.2 SYNTHESIS OF POLY[(VINYLBENZYL)TRIMETHYLAMMONIUM CHLORIDE]

The homopolymer, PVBTMA-Cl was synthesized via RAFT polymerization by using CTPA as a chain transfer agent. The synthesis of was as follows: the monomer, VBTMA-Cl (3.00 g, 14 mmol), and CTPA (36.82 mg, 0.14 mmol) were added to water (15 mL) in 50 mL two-necked round-bottomed flask which was then purged with argon for 45 minutes. The initiator, ACPA (32.2 mg, 0.11 mmol) in water (2 mg/mL) was purged separately and then transferred 4 mL of ACPA solution to the reaction flask under an inert atmosphere. The reaction flask was transferred to the preheated oil bath and conducted the polymerization at 70 °C. Schematic illustration of PVBTMA-Cl synthesis is in Figure 14.

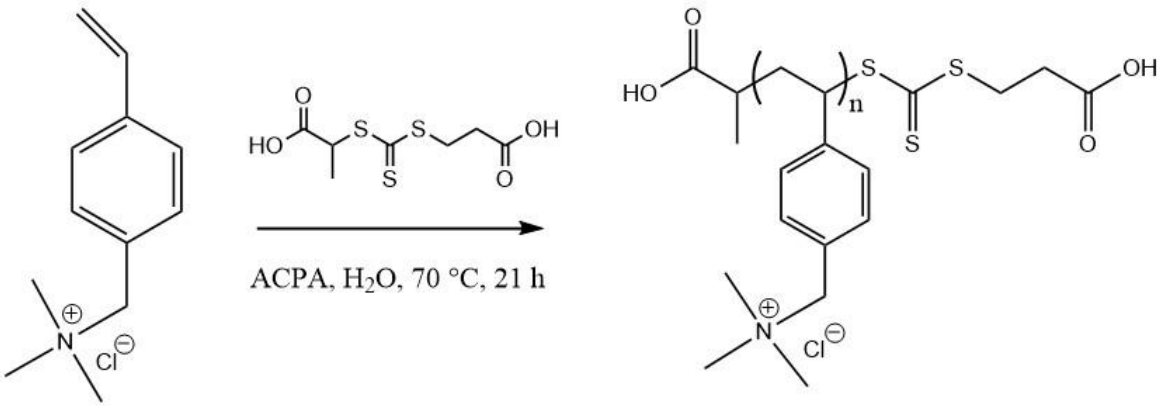

Figure 14. Synthesis of PVBTMA-Cl via RAFT polymerization.

The conversion sample was taken after 16 h reaction time and was analysed with ^{1}H NMR in D_2O. The conversion of monomer was 90% from the NMR and therefore the reaction was stopped after 21 h. The crude PVBTMA-Cl homopolymer was purified by dialysis against water for two days then collected the polymer by freeze-drying the dialyzed solution. The MWCO 6000–8000 $gmol^{-1}$ dialysis tubes were used for the dialysis. The yield of the reaction was 1.86 g.

3.2.3 SYNTHESIS OF BLOCK COPOLYMER

PAA-PVBTMA-Cl block copolymer was synthesized via RAFT polymerization by using PAA macro-CTA as a chain transfer agent. The polymerization was conducted in two conditions; one was in acidic and another was in basic condition. In Figure 15 is the schematic illustration of the synthesis of PAA-PVBTMA-Cl. In a typical synthesis, the same amounts of VBTMA monomer (3.00 g, 14 mmol), PAA macro-CTA (0.52 g, 0.14 mmol) and water (16 mL) were added into the two separate reaction flasks. Then, the first reaction medium was adjusted to the acidic conditions by adding 37% HCl (0.98 g). In the second flask, NaOH (0.40 g) was added to adjust reaction mixture to basic condition. Reaction flasks and ACPA stock solution (2 mg/mL) were purged with argon for 30 minutes. Then the ACPA solution (4 mL) was added into both reaction flasks. Purging was continued 10 minutes and then transferred in an oil bath heated to 70 °C.

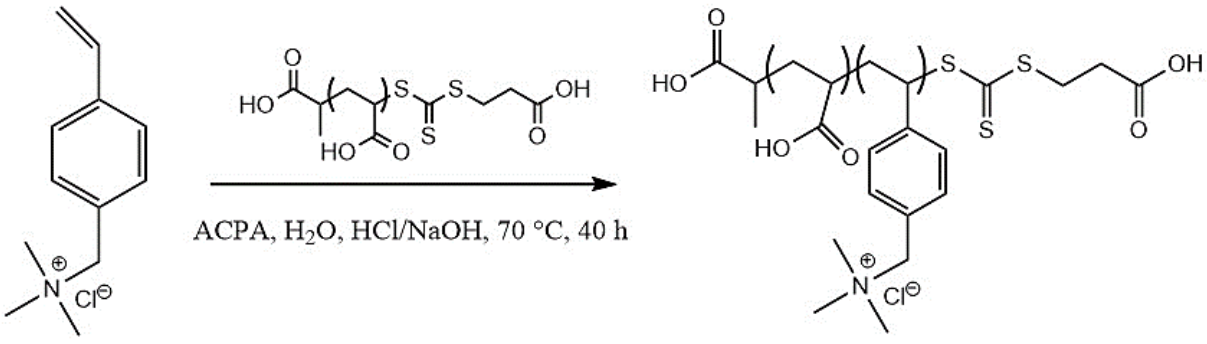

Figure 15. Synthesis of PAA-PVBTMA-Cl via RAFT polymerization.

After 16 h reaction time, the conversion samples were taken and analysed with ^{1}H NMR in D_2O. Both reactions were stopped after 40 h reaction time and second conversion samples were taken. From the second conversion samples, over 90% conversion of monomers was observed

in the sample from acidic medium and about 85% conversion for basic reaction mixture. Crude block copolymers were purified by dialysis against water using 6000–8000 $gmol^{-1}$ dialysis tube for two days by changing the water. Both polymers were collected by freeze-drying the dialyzed solutions. The yield of PAA-PVBTMA-Cl from the acidic reaction was 3.18 g and the basic reaction was 2.87 g.

3.3 CHARACTERIZATION

3.3.1 NMR SPECTROSCOPY

PVBTMA-Cl, PAA macro-CTA, and block copolymer PAA-PVBTMA-Cl were characterized using nuclear magnetic resonance (NMR) spectroscopy. Bruker Avance III 500 MHz spectrometer and one or more of the solvents D_2O, methanol-d_4 (MeOD) and DMSO-d_6 were used for the measurements. In ^{1}H NMR measurements, the polymer concentration was 5 mg/mL, and 100 mg/mL in ^{13}C NMR. The conversions of the monomers were determined by comparing integral values of vinyl signals of monomer to aromatic or carboxylic signals of the polymer by ^{1}H NMR. The molar mass of PAA was determined using end group analysis by comparing signals from CTPA's methyl group (1.05 ppm) to polymer's backbone signals (1.3 – 2.6 ppm).

3.3.2 SIZE EXCLUSION CHROMATOGRAPHY

PAA macro-CTA was characterized with size exclusion chromatography. SEC instrument consists of Waters 515 HPLC pump, Biotech Model 2003 Degasser, Waters 717 plus Autosampler, Waters 2487 Dual λ Absorbance Detector and Waters 2410 Differential Refractometer. Columns consist of Waters Ultrahydrogel 120 and 250, PL aquagel-OH mixed 8 µm and an Ultrahydrogel guard column. The eluent, 0.8 M $NaNO_3$ was used in separation. The flow rate, 0.8 mL/min and 30 °C temperature were maintained during measurements. All samples were dissolved to 0.8 M $NaNO_3$ with a concentration of 2 mg/mL and filtered with PVDF filters. Data were treated with OmniSec 4.7 software. The molar mass of PAA was determined using a standard polyacrylic acid calibration curve, which was measured before the sample.

3.3.3 UV-VIS SPECTROSCOPY

Two different UV-Vis spectroscopies were used in characterization. JASCO J-815 CD spectrometer equipped with a PTC-423S/15 Peltier temperature control system was used to estimate the molar mass of the polymers. The calibration curve for chain transfer agent CTPA in methanol solution was measured at 305 nm wavelength. The molar mass of PAA, PVBTMA-Cl and PAA-PVBTMA-Cl polymer samples were determined by assuming that every single polymer chain has RAFT end group. The calibration concentrations varied from 0.0025 to 0.04 mg/mL and the polymer concentrations varied from 0.25 to 1.0 mg/mL.

The turbidity measurements for block copolymer solutions were conducted by JASCO V-750 UV-Vis spectrophotometer equipped with a JASCO CTU-100 thermostat system. The sample preparation was as follows: the stock solution of the copolymer (20 mg/mL) was prepared 4 days before the dilutions. The dilution samples with 1 mg/mL polymer concentration were prepared by adding the required amount of LiOTf salt at 60 °C. The solution series was made with various LiOTf concentrations 5.0, 7.5, 10.0, 12.5, 15.0, 17.5 and 20.0 mM. The solutions were first degassed below room temperature and then transferred to a sample holder. During the measurements, the samples were first heated to elevated temperatures and then stabilized for 10 minutes. The transmittance of the sample was measured at 600 nm, by first upon cooling the sample solution from 90 °C to 10 °C by collecting temperatures directly from the sample. Then, after 10 minutes of stabilization, the sample was heated from 10 °C to 90 °C. The cooling and heating rates were always 1 °C/min.

3.3.4 POTENTIOMETRIC TITRATION

The potentiometric titrations were conducted for PAA and diblock copolymers using VWR pHenomenal IS 2100 L with a Sentix Mic-B combined pH electrode. pH meter was calibrated using buffer solutions with pH 4, 7 and 10. Sample preparation was as follows: PAA and PAA-PVBTMA-Cl were dissolved to water (0.1 mg/mL and 10 mg/mL respectively). Then to the PAA solution, 0.1 M NaOH was added (2.58×10^{-4} mol) and to the block copolymer solution 0.1 M or 1 M NaOH was added (1.91×10^{-4} mol and 2.58×10^{-4} mol respectively). The PAA and PAA-PVBTMA-Cl solutions were stirred overnight before the titration with 0.1 M HCl.

3.3.5 ZETA POTENTIAL

Malvern Instruments ZetaSizer Nano-ZS equipped with a 4 mW He-Ne laser operating at 633 nm was used to study Zeta potential of the diblock copolymer particles as a function of pH. The pH values were from 2 to 12 with 2 unit increment. The measurements were conducted at 25 °C and voltage were limited to 50 V. Polymer concentration in aqueous solutions was 10 mg/mL.

3.3.6 DYNAMIC LIGHT SCATTERING

Dynamic light scattering (DLS) was used to measure hydrodynamic radii of the diblock copolymer in LiOTf solutions. Samples were measured by a Brookhaven instrument consisting of BI-200SM goniometer, BIC-TurboCorr digital pseudo-cross-correlator, and a BI-CrossCorr detector including two BIC-DS1 detectors. The light source was a Coherent Sapphire 488-100 CDRH laser operating at a wavelength of 488 nm with a 30 mW power. The same samples used for turbidity measurements were measured with this instrument. The solutions were first preheated to elevated temperatures and then filtered to the cuvettes with 0.45 µm PVDF filters. All the measurements were conducted at a 90° angle and the temperature was 25 °C.

In addition, intensity averaged size distributions for PAA-PVBTMA-Cl (1 mg/mL) in 10 mM LiOTf solution were measured as a function of temperature. Malvern Instruments, Zetasizer was used for the measurements. The hydrodynamic radii and scattered intensities were collected at 173° angle by cooling the solution from 80 °C to 20 °C with 5°C step-wise increment. Each temperature was measured three times and the sample was allowed to equilibrate at each temperature for 3 min. In addition, the hydrodynamic radii of diblock copolymers pH solutions discussed above were measured at 25°C.

4. RESULTS AND DISCUSSION

4.1 SYNTHESES AND CHARACTERIZATION OF POLYMERS

4.1.1 SYNTHESES

PAA, PAA-PVBTMA-Cl and PVBTMA-Cl polymers were successfully synthesized via RAFT polymerization. The ratio of [Monomer]:[CTA]:[I] was 50:1:0.2 for PAA and 100:1:0.2 for PVBTMA-Cl and PAA-PVBTMA-Cl syntheses. In diblock copolymer polymerization, the ratio of acid/base to acrylic acid was 1.5. The conversions of the polymerizations were determined by using ^{1}H NMR. End groups of polymers were the same in all polymers, therefore, molar masses of the polymers were determined from UV-Vis spectroscopy by end group analysis. The detailed reaction conditions and molar masses of polymers are reported in Table 1.

Table 1. Reaction conditions and molar masses of polymers.

Polymer	CTA	[M]:[CTA]:[I]	Conv. %	$M_{n(theo)}$	$M_{n(NMR)}$	$M_{n(UV-Vis)}$
PAA	Acid CTA	50:1:0.2	95%	3 680	3 710	5 080
PVBTMA-Cl	Acid CTA	100:1:0.2	95%	20 370	-	29 700
PAA-PVBTMA-Cl	PAA	100:1:0.2	95%	23 820	-	50 230

4.1.2 MOLAR MASS DETERMINATION

Molar masses of polymers were studied using ^{1}H NMR end group analysis. ^{1}H NMR of purified PAA macro-CTA suggested a degree of polymerization 48 which corresponds molar mass 3 710 g/mol. Furthermore, similar results were obtained with SEC where molar mass M_n = 3 540 g/mol and polydispersity index (PDI) 1.274 were obtained. The small difference in molar mass is caused by different methods. SEC is a relative method that needs calibration and therefore standards and eluent can affect results. Acrylic acid was used as a standard and salt solution as an eluent and therefore results are quite reliable. Moreover, the degree of polymerization is close to the targeted value and polymer has a narrow molar mass distribution

which indicates well-controlled RAFT polymerization. In further discussion molar mass 3 710 g/mol is used for PAA. In Appendix 1 are ^{1}H NMR spectra of PAA-PVBTMA-Cl, PVBTMA-Cl, and PAA.

For PVBTMA-Cl and PAA-PVBTMA-Cl polymers, the signals from CTA were overlapped with signals from the backbone and the molar masses could not be determined. However, the composition of the block copolymer was calculated from ^{1}H NMR integral values. The lines used for composition analysis were aromatic signals at 6-8 ppm and the backbone signals at 1-2.6 ppm. Copolymer consists of 70% of VBTMA and 30% of acrylic acid. As macro-CTA had 48 repeating units, the amount VBTMA was estimated to be 112 repeating units which correspond molar mass 27 680 g/mol. However, estimation is only directive and not as accurate as of end-group analysis.

Molar masses of all polymers were determined with UV-Vis spectrometer using the CTA end group for absorbance measurements. In Appendix 2 are absorbance curves of CTA calibration samples and in Figure 16 is the calibration curve of CTA and measured values for PAA, PVBTMA-Cl and PAA-PVBTMA-Cl. From absorbance results, molar masses 5 080, 29 700 and 50 230 g/mol were determined for PAA, PVBTMA-Cl and PAA-PVBTMA-Cl respectively. Molar masses correspond 67 repeating units for PAA, 140 repeating units for PVBTMA-Cl and 218 repeating units of VBTMA in the block copolymer. However, the determined molar masses deviate from theoretical values quite a lot. Furthermore, molar mass measured for PAA using UV-Vis spectroscopy gave molar mass 5 080 g/mol which deviates from ^{1}H NMR and SEC results. Molar mass determination from absorbance measurement is based on the weighted amount of polymer. However, PAA is a hygroscopic material that can affect the results of macro-CTA and block copolymer.[79] Water bonded to PAA increases of a weighted mass of polymer which increases calculated molar mass. Therefore, UV-Vis spectroscopy can give higher molar mass than an actual mass.

4.1.3 POTENTIOMETRIC TITRATION

The amount of acrylic acid in PAA and block copolymer were studied with a back-titration method using an excess amount of NaOH. Neutralization was done overnight to ensure sufficient reaction. Titration experiment indicated 0.138 mmol acrylic acid in PAA which is quite close to theoretical value calculated for macro-CTA with 48 repeating units (0.135 mmol).

In Appendix 3 is an example of a titration curve of PAA. Titrated PAA macro-CTA was purified by dialysis where acrylic acid can dissociate. Dissociation constant pKa for PAA is 4.54 and in pH 7 the fractional number of monomers dissociated (*f*) is 0.32.[80] Thus, in neutral conditions about 30% of the acrylic acid units have been dissociated. Therefore, dissociation of PAA during dialysis can increase the amount of unreacted NaOH which leads to a lower calculated amount of acrylic acid. In addition, the hygroscopic nature of acrylic acid can affect results as discussed above. However, the measured amount of polyacrylic acid is close to the theoretical value and therefore results are quite reliable.

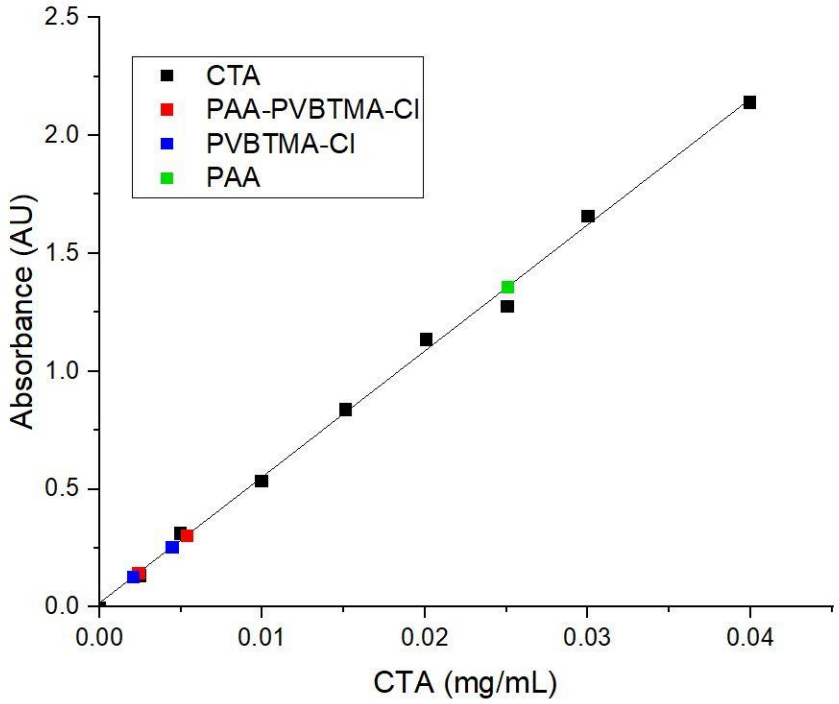

Figure 16. Absorbance as a function of CTA concentration and measured values for PVBTMA-Cl, PAA and PAA-PVBTMA-Cl.

Titration experiments indicated 0.09 mmol acrylic acid in block copolymer which corresponds 17% of AA in the copolymer. It corresponds 48 repeating units of AA and 234 repeating units of VBTMA-Cl which is close to molar mass 53 500 g/mol. However, calculated repeating units and molar masses are only directive ones. Figure 17 is an example of the titration curve of the block copolymer. Comparing potentiometric titration results to ^{1}H NMR results shows deviation. ^{1}H NMR results suggested that molar ratio would be 70% of VBTMA and 30% of AA whereas titration results indicated that molar ratio would be 83% and 17%. The deviation

between ^{1}H NMR and titration results can be affected by the hygroscopic nature of block copolymer. In the case of titration, the composition is calculated based on a weighted mass of copolymer whereas in NMR composition is calculated based on integral values of lines. Therefore, water bonded to block copolymer can increase the molar ratio of VBTMA in the copolymer. In addition, acrylic acid groups were partially dissociated during purification as discussed above. A higher amount of unreacted NaOH leads to a lower amount of acrylic acid which affects the calculated molar ratio. Thus, dissociation of acid groups and hygroscopic nature of block copolymer can decrease the molar ratio of AA in block copolymer and it is possible that ^{1}H NMR results are more accurate. Therefore, in further discussion molar ratio of 70% of VBTMA and 30% of AA is used.

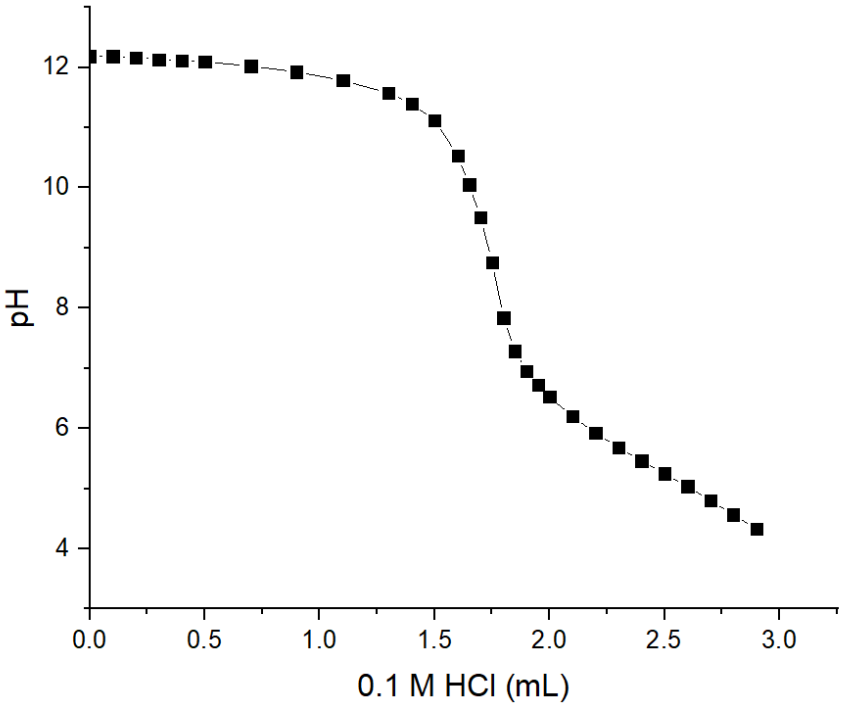

Figure 17. Titration curve of PAA-PVBTMA-Cl.

4.1.4 ^{13}C NMR

^{13}C NMR was measured for PVBTMA-Cl and PAA-PVBTMA-Cl and spectra are seen in **Virhe. Viitteen lähdettä ei löytynyt.**. The spectrum of PVBTMA-Cl showed characteristic signals for cationic polymer however, compared to diblock copolymer's spectrum big differences are not seen. The carboxylic acid signal is not seen in the spectrum even though two

different solvents were used (D_2O, MeOD). One reason could be the conformation of block copolymer chains. Acrylic acid groups are partially dissociated in block copolymer solution. This can lead to higher hydrophobic nature compared to a cationic block where all groups are charged in all conditions. More hydrophobic nature of acrylic acid can induce core-corona structure where more hydrophobic acrylic acid is in core and more hydrophilic VBTMA-Cl is in the corona.[19,68] Thus, acrylic acid is screened by VBTMA-Cl and cannot be detected by ^{13}C NMR. Another possibility is that measurement conditions affect characterization with ^{13}C NMR and change of conditions could show the PAA signals.

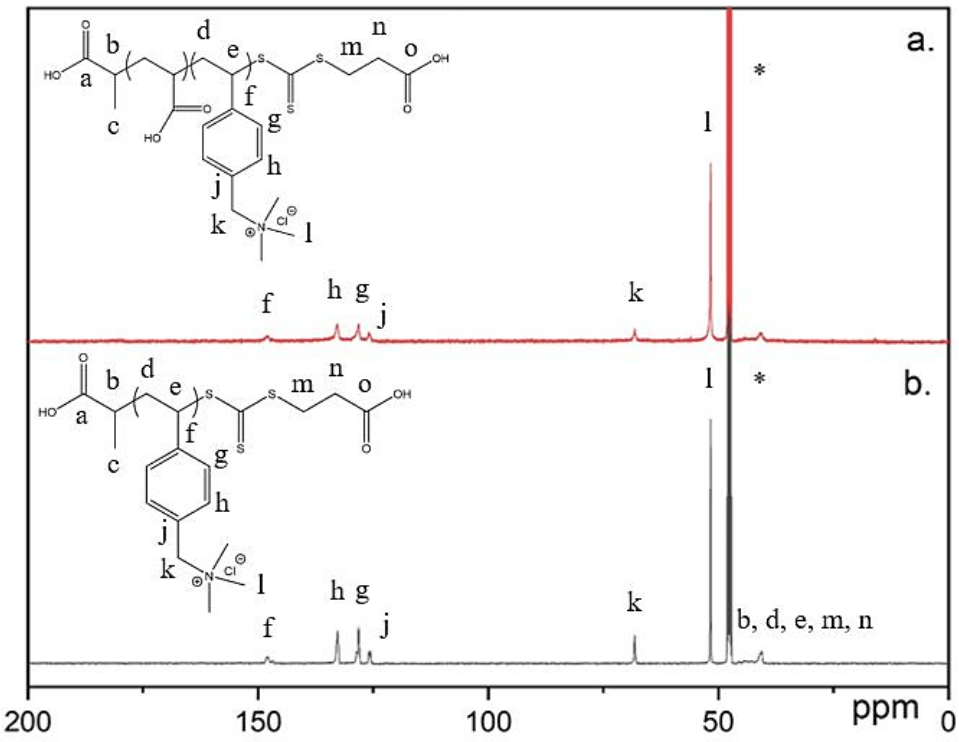

Figure 18. ^{13}C NMR spectra of a) PAA-PVBTMA-Cl and b) PVBTMA-Cl in MeOD.

4.2 SOLUTION PROPERTIES

4.2.1 SALT SOLUTIONS

The solubility of PAA-PVBTMA-Cl polymer was studied in different salt solutions. Addition of NaCl, NaOH and LiOTf made solutions opaque. With an increasing amount of NaCl or LiOTf turbidity increased until polymer particles were unstable and precipitated slowly at room temperature. Cloudy salt solutions are consistent with the literature. Baddam *et al.*[18] had

PVBTMA-OTf homopolymer which turned cloudy in LiOTf solution. In addition, LiOTf solution made homopolymer thermoresponsive with UCST sort of behaviour.[18] Therefore, PAA-PVBTMA-Cl LiOTf solutions were studied further to characterize solution properties and possible UCST type of behaviour.

4.2.2 ZETA POTENTIAL

Block copolymer solution (10 mg/mL) was studied by zeta sizer at pH range from 2 to 12. Zeta sizer results showed that polymer had always positive surface charge and it did not depend on the pH of the solution. Figure 19 shows the zeta potential as a function of pH. Zeta sizer results indicated that PAA-PVBTMA-Cl block copolymer has a micellar structure which is not switchable with the used molar ratios. Acrylic acid stays in the core of micelles in whole pH range and therefore surface charge of micelles stays positive. This observation is in line with the ^{13}C NMR result where the acrylic acid signal could not be detected. In addition, PAA-PVBTMA-Cl has a quite asymmetrical block ratio (48:112) which affects the formation of reverse micelle.

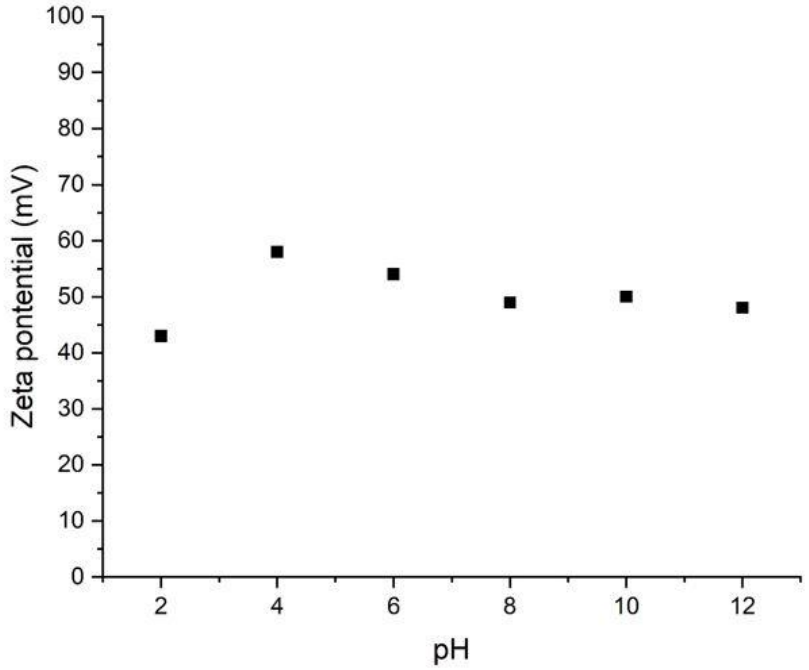

Figure 19. Zeta potential for PAA-PVBTMA-Cl as a function of pH.

According to Bütün *et al.*[67] asymmetric block copolymers do not form easily stable reverse micelles and formation of reverse micelles needs careful control of temperature. With a higher amount of AA, it might be possible to obtain anionic micelles where VBTMA would be in the core and AA in the corona. However, VBTMA-Cl is a strong polyelectrolyte and formation of a hydrophobic core with strong polyelectrolyte is difficult and would possibly need hydrophobic salt which would condense on the cation. However, further studies are needed to show schizophrenic behaviour for PAA-PVBTMA-Cl.

4.2.3 TURBIDIMETRY

The transmittance of block copolymer solution (1 mg/mL) was studied as a function of LiOTf concentration from 5 to 20 mM. Block copolymer solutions were first cooled from 90 to 10 °C and then heated back to 90 °C. Results of cooling measurements are in Figure 20. Solutions were clear in higher temperatures and turned turbid in lower temperatures which could be an indication of UCST type of behaviour. However, the concentration of LiOTf affected behaviour drastically. In the 5 mM solution, no turbidity changes were observed. Increasing LiOTf concentration increased transmittance changes and for 20 mM solution, quite clear change from clear to turbid solution was observed. However, change from the clear to the turbid solution was gradual and clear cloud points could not be obtained. In higher LiOTf concentrations turbidity changed more rapidly than in lower concentrations. Therefore, it might be possible to obtain clear cloud points for block copolymer by adjusting the amount of salt in solutions.

Karjalainen *et al.*[9] have shown that hydrophobic OTf anion can induce UCST type of behaviour in cationic polymers. However, ionic strength must be high enough with high enough counterion concentration to induce thermoresponsive behaviour.[9] In addition, Baddam *et al.*[18] polymerized PVBTMA-OTf homopolymer and PEG-PVBTMA-OTf block copolymer and both showed UCST type of behaviour. Moreover, it was shown that partially neutralized polyacrylic acid can have a UCST type of behaviour in high ionic strength solutions.[81] Therefore, ionic strength in PAA-PVBTMA-Cl LiOTf solutions was too low to induce clear UCST type of behaviour and clear cloud points. However, a higher concentration of OTf precipitated polymer particles. Therefore, ionic strength should be increased with salt which has no hydrophobic character, for example with NaCl. The pH of the solution can affect UCST sort of behaviour due to dissociation of acrylic acid. Therefore, more basic solution conditions

could induce clearer UCST-type behaviour. Thus, solution conditions need further adjustment to show clear cloud points. In Figure 21 are pictures of clear and turbid block copolymer LiOTf solutions.

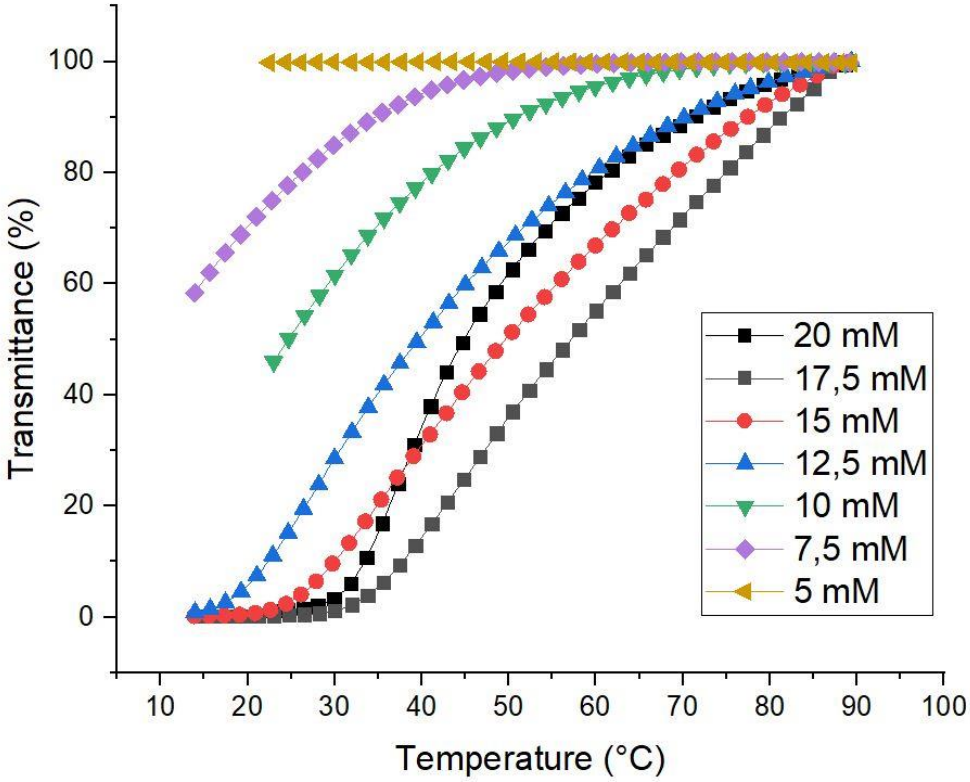

Figure 20. Transmittance measured during cooling of PAA-PVBTMA-Cl (1 mg/mL) with LiOTf concentration from 5 to 20 mM.

Thermoresponsive behaviour was studied by cross-experiment where PAA and PVBTMA-Cl homopolymers were mixed together with same molar ratios as in block copolymer. Into polymer solution was introduced LiOTf to induce UCST type of behaviour. However, the homopolymer mixture formed strong complexes and did not show the UCST type of behaviour at temperature range 20 – 90 °C. This indicates that block copolymer does not only contain physical interactions between acrylic acid and VBTMA-Cl but also the two blocks are covalently bound to each other. Therefore, copolymer shows thermoresponsive behaviour in the presence of LiOTf salt.[18]

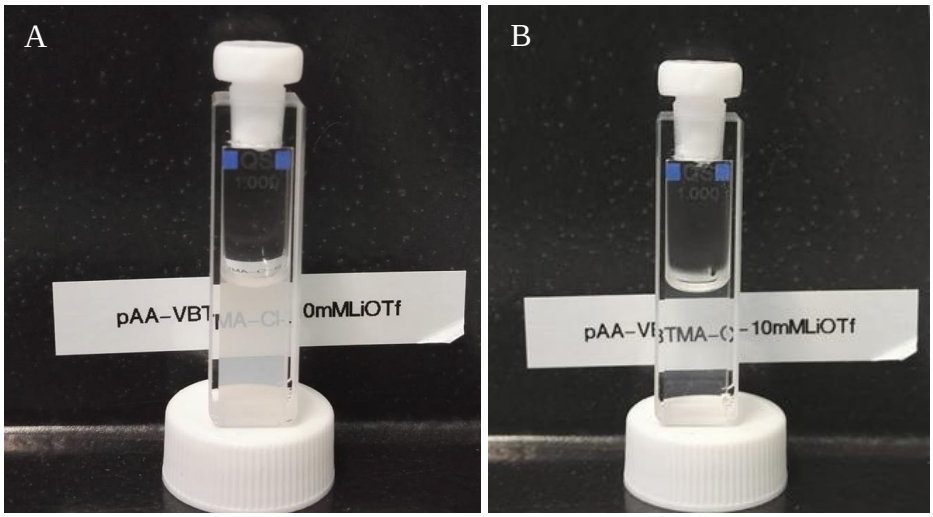

Figure 21. PAA-PVBTMA-Cl (1 mg/mL) solution with 10 mM LiOTf a) at room temperature and b) at 90 °C.

4.2.4 DLS

Block copolymer solutions (1 mg/mL in 5 – 20 mM LiOTf solution) were studied with DLS and results are in Figure 22. DLS results indicated that the size of particles increases with increasing LiOTf concentration. When the salt concentration was over 20 mM block copolymer precipitated. When no salt was added polymer dissolved molecularly. Thus, the addition of hydrophobic OTf anion made block copolymer more hydrophobic and increasing amount of salt made polymer to aggregate. Aggregates grew with an increasing amount of LiOTf and finally, polymer particles were unstable and precipitated.

According to literature, aggregation of the diblock copolymer is caused by interactions between salt and polymer.[18,82] Addition of LiOTf salt to copolymer solution screens cationic charges and decreases the repulsive interactions. Thus, the diblock copolymer can form core-corona conformation where acrylic acid is inside the core. Higher LiOTf concentration leads to bigger aggregates due to increased hydrophobicity of block copolymer and after threshold value polymer precipitates.

In addition, DLS measurements were made with block copolymer (1 mg/mL) in 10 mM LiOTf solution at 20 – 80 °C using backscattering angle θ = 173° and results are in Figure 23. Results indicated that the size of particles decreases with increasing temperature. However, polymer particles did not disappear even at 80 °C which is an indication of incomplete dissolution. Polymer particles did not dissolve molecularly at high temperatures even though block

copolymer dissolved molecularly to pure water at room temperature. Results showed that particle size decreased from 350 to 180 nm, however, big aggregates were not detected during measurement.

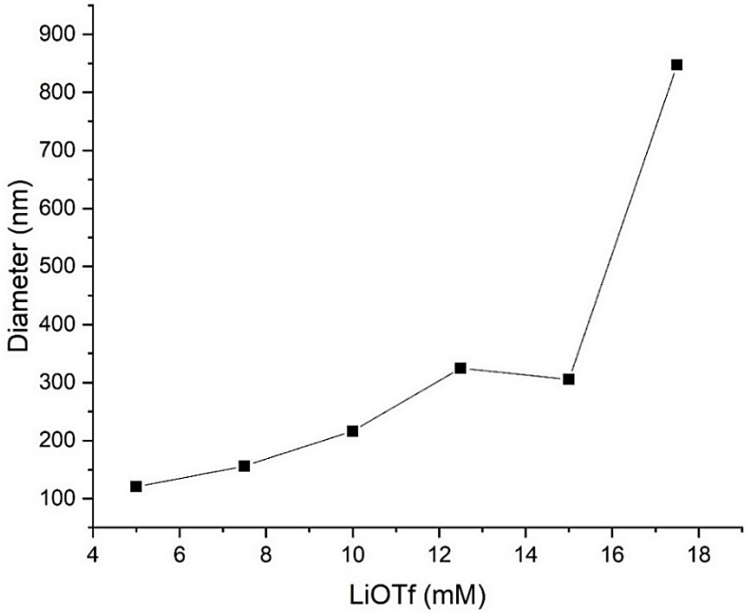

Figure 22. The hydrodynamic diameter of PAA-PVBTMA-Cl diblock copolymer as a function of LiOTf concentration.

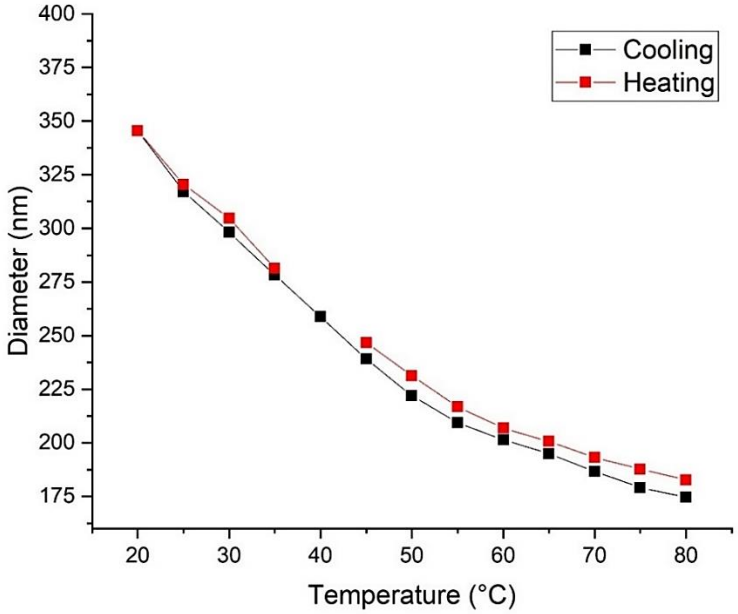

Figure 23. The hydrodynamic diameter of PAA-PVBTMA-Cl in 10 mM LiOTf solution as a function of temperature.

Decreasing particle size during heating can be an indication of the UCST type of behaviour. Block copolymer size decreased gradually during heating and no fast particle size changes were observed. This observation is in line with transmittance measurements where turbidity decreased gradually. Therefore, it is possible that increasing ionic strength in solution would induce a sharper change in particle size as discussed above. However, DLS temperature measurements were only done for one sample. More studies are needed to give reliable conclusions about polymer solution behaviour.

CONCLUSIONS

Syntheses of the polymers were successful via RAFT polymerization. PAA macro-CTA, with narrow molar mass distribution and well-defined molar mass, was further employed in the synthesis of the diblock copolymer. The PAA-PVBTMA-Cl copolymer composition, 30% of AA and 70% VBTMA were determined with ^{1}H NMR, which is close to the targeted value (33% of AA and 67% of VBTMA). In addition, PVBTMA-Cl homopolymer was synthesized via RAFT polymerization for comparative studies. The characterization of molar mass with ^{1}H NMR was not possible as the proton signals from CTA end groups overlapped with polymer backbone signals. Instead molar masses were determined with UV-Vis spectroscopy. In further studies, one could verify well-controlled polymerization by kinetic analysis.

The Zeta potential measurements indicated that diblock copolymer has a micellar structure in salt solutions. Further, turbidity and DLS measurements showed that diblock copolymer has a UCST type of behaviour in LiOTf solutions. However, solution conditions must be adjusted to higher ionic strength to get clear cloud points. There were no turbidity changes observed for the mixture of two homopolymers (PAA and PVBTMA-Cl) in LiOTf solutions. This result indicated that in the block copolymer the complexation of two blocks was somehow controlled and the blocks are covalently bound to each other.

Schizophrenic behaviour was not observed in the diblock copolymer and polymer micelles had only a positive surface charge. However, with symmetric block ratio and careful selection of solution conditions, it can be possible to induce schizophrenic micelles in different pH conditions. Further studies are needed to characterize all solution properties of the diblock copolymer with varying the block compositions.

REFERENCES

1 A. B. Lowe and C. L. McCormick, *Chem. Rev.*, 2002, **102**, 4177-4190.

2 J. Nicolas, Y. Guillaneuf, C. Lefay, D. Bertin, D. Gigmes and B. Charleux, *Prog. Polym. Sci.*, 2013, **38**, 63-235.

3 K. Matyjaszewski, *Adv. Mater.*, 2018, **30**, 1706441.

4 G. Moad, *Polym. Chem.*, 2017, **8**, 177-219.

5 A. M. Caltabiano, J. P. Foley and A. M. Striegel, *J. Chromatogr. A*, 2018, **1532**, 161-174.

6 G. J. M. Koper and M. Borkovec, *Polymer*, 2010, **51**, 5649-5662.

7 V. Bütün, S. Liu, J. V. M. Weaver, X. Bories-Azeau, Y. Cai and S. P. Armes, *React. Funct. Polym.*, 2006, **66**, 157-165.

8 Y. Kawata, S. Kozuka and S. Yusa, *Langmuir*, 2019, **35**, 1458-1464.

9 E. Karjalainen, V. Aseyev and H. Tenhu, *Macromolecules*, 2014, **47**, 7581-7587.

10 Q. Chen, J. Zheng, X. Yuan, J. Wang and L. Zhang, *Mater. Sci. Eng. C*, 2018, **82**, 1-9.

11 K. T. P. Charan, N. Pothanagandhi, K. Vijayakrishna, A. Sivaramakrishna, D. Mecerreyes and B. Sreedhar, *Eur. Polym. J.*, 2014, **60**, 114-122.

12 C. Karlsson and P. Jannasch, *ACS Appl. Energy Mater.*, 2019, **2**, 6841-6850.

13 Y. Tian, X. Wei, Z. J. Wang, P. Pan, F. Li, D. Ling, Z. L. Wu and Q. Zheng, *ACS Appl. Mater. Interfaces*, 2017, **9**, 34349-34355.

14 J. Choi and M. F. Rubner, *Macromolecules*, 2005, **38**, 116-124.

15 C. Tanford, *Physical Chemistry of Macromolecules*, John Wiley & Sons Inc., USA, 1961.

16 F. Wang, J. Yang and J. Zhao, *Polym. Int.*, 2015, **64**, 999-1005.

17 B. Saha, N. Choudhury, A. Bhadran, K. Bauri and P. De, *Polym. Chem.*, 2019, **10**, 3306-3317.

18 V. Baddam, V. Aseyev, S. Hietala, E. Karjalainen and H. Tenhu, *Macromolecules*, 2018, **51**, 9681-9691.

19 S. L. Canning, T. J. Neal and S. P. Armes, *Macromolecules*, 2017, **50**, 6108-6116.

20 L. Martin, G. Gody and S. Perrier, *Polym. Chem.*, 2015, **6**, 4875-4886.

21 M. Sponchioni, U. C. Palmiero, N. Manfredini and D. Moscatelli, *React. Chem. Eng.*, 2019, **4**, 436-446.

22 Z. Iatridi, M. M. S. Lencina and C. Tsitsilianis, *Polym. Chem.*, 2015, **6**, 3942-3955.

23 S. Fang, G. Wang, P. Li, R. Xing, S. Liu, Y. Qin, H. Yu, X. Chen and K. Li, *Int. J. Biol. Macromol.*, 2018, **115**, 754-761.

24 S. Perrier, *Macromolecules*, 2017, **50**, 7433-7447.

25 L. Michalek, L. Barner and C. Barner-Kowollik, *Adv. Mater.*, 2018, **30**, 1706321.

26 W. Xu, P. A. Ledin, V. V. Shevchenko and V. V. Tsukruk, *ACS Appl. Mater. Interfaces*, 2015, **7**, 12570-12596.

27 H. Charaya, X. Li, N. Jen and H. Chung, *Langmuir*, 2019, **35**, 1526-1533.

28 A. Skandalis and S. Pispas, *J. Polym. Sci., Part A: Polym. Chem.*, 2019, **57**, 1771-1783.

29 R. C. van Duijvenbode, A. Rajanayagam, G. J. M. Koper, M. W. P. L. Baars, B. F. M. de Waal, E. W. Meijer and M. Borkovec, *Macromolecules*, 2000, **33**, 46-52.

30 G. Gody, T. Maschmeyer, P. B. Zetterlund and S. Perrier, *Nat. Commun.*, 2013, **4**, 2505.

31 D. R. Carroll, A. P. Constantinou, N. Stingelin and T. K. Georgiou, *Polym. Chem.*, 2018, **9**, 3450-3454.

32 *Acrylic Acid, A Summary of Safety and Handling, 4th ed.*, 2013, http://msdssearch.dow.com/PublishedLiteratureDOWCOM/dh_0933/0901b80380933166.pdf?filepath=acrylates/pdfs/noreg/745-00006.pdf&fromPage=GetDoc, (accessed 10/14 2019).

33 F. Oosawa, *Polyelectrolytes*, Marcel Dekker, Inc., New York, 1971.

34 A. Kundagrami and M. Muthukumar, *Macromolecules*, 2010, **43**, 2574-2581.

35 A. V. Dobrynin and M. Rubinstein, *Prog. Polym. Sci.*, 2005, **30**, 1049-1118.

36 K. Zheng, K. Chen, W. Ren, J. Yang and J. Zhao, *Macromolecules*, 2018, **51**, 4444-4450.

37 I. Kagawa and K. Katsuura, *J. Polym. Sci.*, 1955, **17**, 365-374.

38 R. A. Marcus, *J. Phys. Chem.*, 1954, **58**, 621-623.

39 A. Katchalsky, J. Mazur and P. Spitnik, *J. Polym. Sci.*, 1957, **23**, 513-532.

40 R. G. Smits, G. J. M. Koper and M. Mandel, *J. Phys. Chem.*, 1993, **97**, 5745-5751.

41 G. S. Manning, *J. Chem. Phys.*, 1969, **51**, 924.

42 J. Lipfert, S. Doniach, R. Das and D. Herschlag, *Annu. Rev. Biochem.*, 2014, **83**, 813-841.

43 R. M. Fuoss and U. P. Strauss, *J. Polym. Sci.,* 1948, **3**, 602-603.

44 P. Munk, in *Introduction to Macromolecular Science,* A Wiley-Interscience publication, New York, 1989, 59.

45 F. Ascoli and C. Botré, *J. Polym. Sci.,* 1962, **62**, 56-59.

46 Y. Kantor, H. Li and M. Kardar, *Phys. Rev. Lett.,* 1992, **69**, 61.

47 A. D. McNaught and A. Wilkinson, in *IUPAC. Compendium of Chemical Terminology, 2nd ed. (the Gold Book), online version,* https://goldbook.iupac.org/, (accessed 09/17 2019*),* Blackwell Scientific Publications, Oxford, 1997.

48 F. G. Donnan and A. B. Harris, *J. Chem. Soc., Trans.,* 1911, **99**, 1554-1577.

49 P. Atkins and J. Paula, in *Atkins' Physical Chemistry, 10th ed.*, Oxford University Press, 2014, 199-200.

50 F. G. Donnan, *Chem. Rev.,* 1924, **1**, 73-90.

51 M. Vis, V. F. D. Peters, R. H. Tromp and B. H. Erné, *Langmuir,* 2014, **30**, 5755-5762.

52 M. K. Georges, R. P. N. Veregin, P. M. Kazmaier and G. K. Hamer, *Macromolecules,* 1993, **26**, 2987-2988.

53 C. J. Hawker, A. W. Bosman and E. Harth, *Chem. Rev.*, 2001, **101**, 3661-3688.

54 M. Kato, M. Kamigaito, M. Sawamoto and T. Higashimura, *Macromolecules,* 1995, **28**, 1721-1723.

55 J. Wang and K. Matyjaszewski, *J. Am. Chem. Soc.*, 1995, **117**, 5614-5615.

56 J. Chiefari, Y. K. Chong, F. Ercole, J. Krstina, J. Jeffery, T. P. T. Le, R. T. A. Mayadunne, G. F. Meijs, C. L. Moad, G. Moad, E. Rizzardo and S. H. Thang, *Macromolecules,* 1998, **31**, 5559-5562.

57 S. Perrier and P. Takolpuckdee, *J. Polym. Sci., Part A: Polym. Chem.*, 2005, **43**, 5347-5393.

58 S. L. Canning, G. N. Smith and S. P. Armes, *Macromolecules,* 2016, **49**, 1985-2001.

59 G. Gody, T. Maschmeyer, P. B. Zetterlund and S. Perrier, *Macromolecules,* 2014, **47**, 639-649.

60 L. Zhang and A. Eisenberg, *Science,* 1995, **268**, 1728-1731.

61 S. Kudaibergenov, J. Koetz and N. Nuraje, *Adv. Compos. Hybrid Mater.*, 2018, **1**, 649-684.

62 C. M. Papadakis, P. Müller-Buschbaum and A. Laschewsky, *Langmuir,* 2019, **35**, 9660-9676.

63 S. Liu and S. P. Armes, *Angew. Chem., Int. Ed.,* 2002, **41**, 1413-1416.

64 D. Wang, T. Wu, X. Wan, X. Wang and S. Liu, *Langmuir,* 2007, **23**, 11866-11874.

65 K. Vijayakrishna, D. Mecerreyes, Y. Gnanou and D. Taton, *Macromolecules,* 2009, **42**, 5167-5174.

66 A. Blanazs, S. P. Armes and A. J. Ryan, *Macromol. Rapid Commun.,* 2009, **30**, 267-277.

67 V. Bütün, N. C. Billingham and S. P. Armes, *J. Am. Chem. Soc.,* 1998, **120**, 11818-11819.

68 A. Ghamkhari, B. Massoumi and M. Jaymand, *Des. Monomers Polym.,* 2017, **20**, 190-200.

69 J. V. M. Weaver, S. P. Armes and V. Bütün, *Chem. Commun.,* 2002, 2122-2123.

70 N. S. Vishnevetskaya, V. Hildebrand, N. M. Nizardo, C. Ko, Z. Di, A. Radulescu, L. C. Barnsley, P. Müller-Buschbaum, A. Laschewsky and C. M. Papadakis, *Langmuir,* 2019, **35**, 6441-6452.

71 S. Liu, N. C. Billingham and S. P. Armes, *Angew. Chem., Int. Ed.,* 2001, **40**, 2328-2331.

72 C. Zhao, Z. Ma and X. X. Zhu, *Prog. Polym. Sci.,* 2019, **90**, 269-291.

73 M. Heskins and J. E. Guillet, *J. Macromol. Sci. -Chem.,* 1968, **2**, 1441-1455.

74 H. C. Haas and N. W. Schuler, *J. Polym. Sci., Part B: Polym. Lett.,* 1964, **2**, 1095-1096.

75 D. N. Schulz, D. G. Peiffer, P. K. Agarwal, J. Larabee, J. J. Kaladas, L. Soni, B. Handwerker and R. T. Garner, *Polymer,* 1986, **27**, 1734-1742.

76 F. Liu, J. Seuring and S. Agarwal, *J. Polym. Sci., Part A: Polym. Chem.,* 2012, **50**, 4920-4928.

77 V. Baddam, R. Missonen, S. Hietala and H. Tenhu, *Macromolecules,* 2019, **52**, 6514-6522.

78 K. K. Sharker, Y. Ohara, Y. Shigeta, S. Ozoe and S. Yusa, *Polymers,* 2019, **11**, 265.

79 K. Hiraoka and T. Yokoyama, *Polym. Bull.,* 1980, **2**, 183-188.

80 T. Swift, L. Swanson, M. Geoghegan and S. Rimmer, *Soft Matter,* 2016, **12**, 2542-2549.

81 P. J. Flory and J. E. Osterheld, *J. Phys. Chem.,* 1954, **58**, 653-661.

82 Y. Biswas, T. Maji, M. Dule and T. K. Mandal, *Polym. Chem.,* 2016, **7**, 867-877.

APPENDIX

Appendix 1. 1H NMR spectra of a) PAA-PVBTMA-Cl b) PVBTMA-Cl and c) PAA.

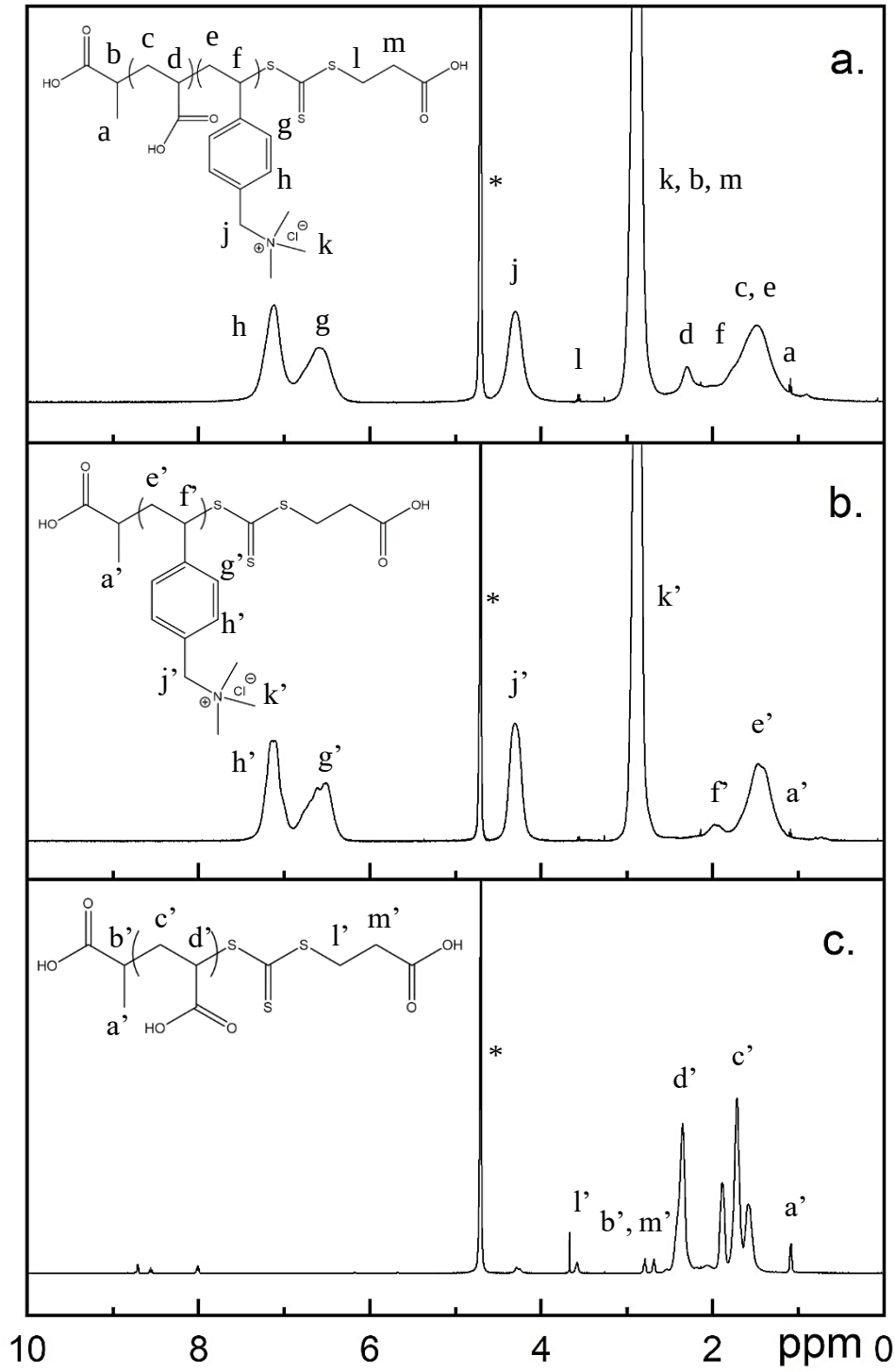

Appendix 2. Absorbance curves of CTA calibration.

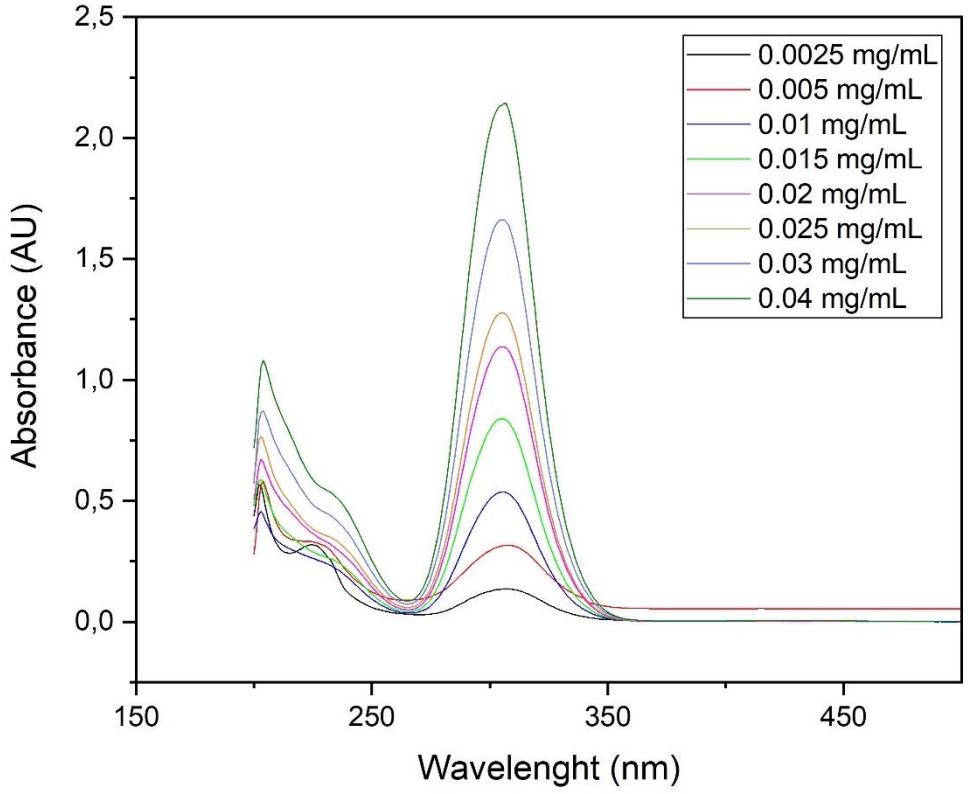

Appendix 3. Titration curve of PAA with 0.1 M HCl.